Journal of Marine Systems 83 (2010) 192–209

Contents lists available at ScienceDirect

Journal of Marine Systems

journal homepage: www.elsevier.com/locate/jmarsys

The role of inorganic nutrients and dissolved organic phosphorus in the phytoplankton dynamics of a Mediterranean bay
A modeling study

Clara Llebot [a,*], Yvette H. Spitz [b], Jordi Solé [a], Marta Estrada [a]

[a] Institut de Ciències del Mar, CSIC, Passeig Marítim de la Barceloneta 37-49, 08003 Barcelona, Spain
[b] College of Oceanic and Atmospheric Sciences, Oregon State University, 104 COAS Administration Building, Corvallis, OR, USA

ARTICLE INFO

Article history:
Received 15 October 2009
Received in revised form 16 June 2010
Accepted 18 June 2010
Available online 28 June 2010

Keywords:
Spain
Catalunya
Alfacs Bay
Mediterranean Sea
Dissolved organic phosphorus
Resuspended sediments
Ecological modeling
Phytoplankton
Limiting factors

ABSTRACT

The effect of Dissolved Organic Phosphorus (DOP) availability and nutrient limitation of phytoplankton growth in an estuarine bay (Alfacs Bay, NW Mediterranean) have been studied by means of a zero-dimensional ecological model including nitrogen, phosphorus (organic and inorganic), two groups of phytoplankton (diatoms and flagellates), one group of zooplankton, and detritus. Simulations with and without DOP as an extra source of phosphorus for phytoplankton growth suggest that DOP plays an important role in the dynamics of the Alfacs Bay ecosystem. DOP is indeed necessary to simulate the observed draw-down of nitrate and build up of phytoplankton biomass. Two non-exclusive mechanisms allowing DOP availability for phytoplankton are possible: direct uptake, or remineralization to Dissolved Inorganic Phosphorus. Including both gives a better agreement with the observations. Inclusion of DOP in the model leads to predominance of phosphorus limitation of phytoplankton growth in fall and winter, and of nitrogen limitation in late spring and summer. Simulations with and without sediment resuspension suggest that this process does not significantly affect the nutrient budget in the bay.

1. Introduction

Coastal regions are highly dynamic and productive areas that have historically attracted human populations. In the confluence between a river mouth and the sea, estuaries hold a variety of habitats and have both a high ecological and economic value. Such areas process nutrients as they pass from the land to the sea, provide shelter and nursery grounds for many aquatic species, and support successful fisheries and aquaculture activities.

A major challenge in the study of marine coastal areas is understanding the interactions among physico-chemical variables and ecosystem behavior. Alfacs Bay represents a good case study for this challenge. Alfacs (NW Mediterranean, Fig. 1) is a shallow bay (3.13 m deep on average) characterized by human controlled freshwater discharge and subject to the typically small tides of the Mediterranean (less than 0.2 m). It is highly productive, and hosts successful aquaculture businesses (Camp and Delgado, 1987; DAAAR, 2008). However, algal blooms – some of them harmful – have been recurrent in Alfacs since 1989 (Delgado et al., 1990). Harmful algal blooms (HABs) consist of different species, such as the dinoflagellates *Alexandrium minutum* (Delgado et al., 1990), *Dinophysis sacculus* (Garcés et al., 1997) and *Karlodinium spp.* (formerly identified as *Gyrodinium corsicum*) (Garcés et al., 1999; Fernández-Tejedor et al., 2004), and diatoms of the genus *Pseudonitzschia* (Quijano-Sheggia et al., 2008). Their frequency has increased over the years, just as it has increased in other harbors of the neighboring Catalan coast (Vila et al., 2001). Some of these proliferations are associated with massive mortalities of cultured fish, and others cause mussel (*Mytillus galloprovincialis*) toxicity for humans (due to Diarrhetic or Paralytic Shellfish Poisoning). Because these blooms consist primarily of flagellates or diatoms, the dynamics of these groups and nutrient control of their populations will be one of the foci of this study.

The main sources of dissolved inorganic nutrients in Alfacs Bay are freshwater discharge from irrigation channels and treatment plants (Camp, 1994), ground water input, exchange with the open ocean through the mouth of the bay, flux from sediments (Delgado and Camp, 1987; Vidal, 1994), and recycling and remineralization from biological processes. Agricultural practice in the Ebre Delta, which is dominated by rice farming, delivers high inorganic nitrogen loads to the bay (of the order of 20–100 mmol N m^{-3}) through freshwater drainage channels. In general June and October are the months with

* Corresponding author. Tel.: +01 5417379092.
E-mail addresses: cllebot@coas.oregonstate.edu (C. Llebot), yvette@coas.oregonstate.edu (Y.H. Spitz), jsole@icm.cat (J. Solé), marta@icm.cat (M. Estrada).

0924-7963/$ – see front matter © 2010 Elsevier B.V. All rights reserved.
doi:10.1016/j.jmarsys.2010.06.009

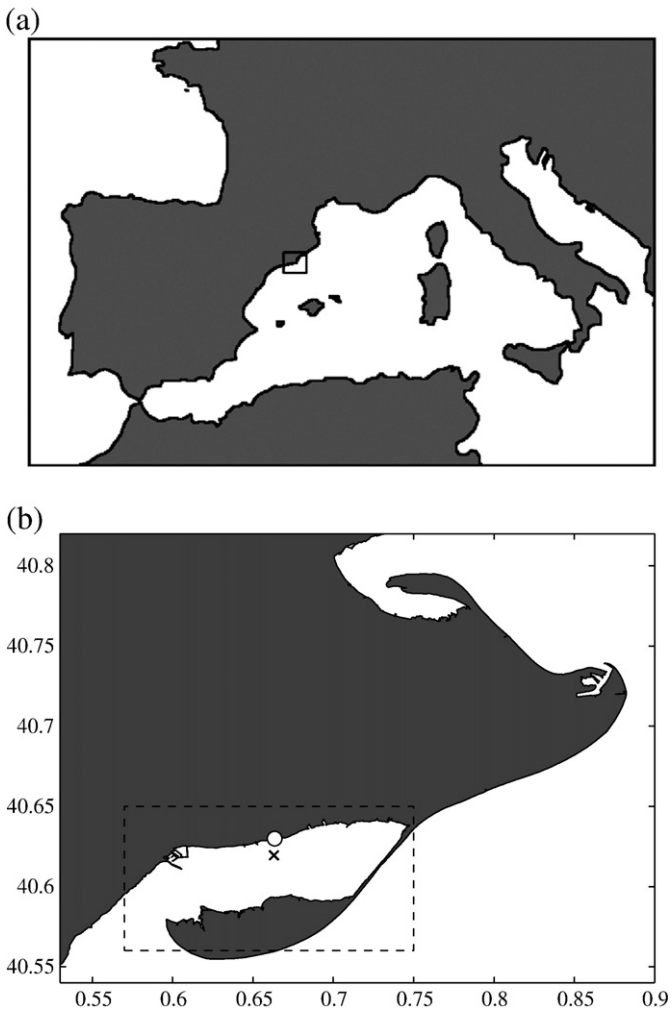

Fig. 1. Map of the study zone in Latitude/Longitude coordinates. - - Els Alfacs Bay; ○: weather station; x: sampling site.

higher nutrient concentration in the channels, because the fields are fertilized in June and emptied in October after the crop (Muñoz, 1998). Phosphorus concentrations are generally low (0.5–1.5 mmol P m^{-3}). In addition to drainage channels, ground water seepage appears to be also an important source of nutrients, given the high nitrate concentrations in the Ebre Delta aquifers, where up to 1500 mmol N m^{-3} have been reported (Ministerio de Obras Públicas, Transportes y Medio Ambiente; Ministerio de Industria y Energía, 1995; Torrecilla et al., 2005). The main nutrient sinks are exchanges with the sea and consumption by phytoplankton, which can also produce detrital matter sinking to the sediment. In addition to dissolved inorganic nutrients, dissolved organic compounds have been found in high concentration in the bay, in association with freshwater discharge. Recent studies (Loureiro et al., 2009) have documented much higher concentrations of dissolved organic phosphorus than of inorganic phosphorus concentrations during the summer.

In spite of previous work on the linkage between the phytoplankton community and the physics in Alfacs Bay (Artigas, 2008; Llebot et al., 2008), a good understanding of the main physico-chemical factors controlling the phytoplankton community is still lacking. One outstanding question concerning the ecology of Alfacs Bay is the role of nutrient fluxes on phytoplankton community succession and bloom development. Nutrient control of phytoplankton growth in Alfacs Bay has been addressed by several field studies, but with contrasting results. On one hand, Delgado and Camp (1987) reported a N:P ratio between 0.2 and 10.2, and by comparison with Redfield ratio concluded that nitrogen was the limiting nutrient of the system. On the other hand, Cruzado et al. (2002) found that phosphorus was the limiting nutrient in the Ebre Delta system and attributed this observation to the contribution of freshwater discharge, which is high in nitrogen and low in phosphorus. Freshwater input to Alfacs is indeed low in phosphorus due to its retention in the rice fields, as observed by Forès (1989). Finally, other studies point to a more complicated situation of alternating phosphorus and nitrogen limitation. Vidal (1994) considered that phosphorus was the main limiting nutrient for phytoplankton growth in Alfacs, but suggested that atmospheric and hydrodynamic forces could play key roles in alternating nitrogen and phosphorus limitation. Quijano-Sheggia et al. (2008) found that inorganic P limitation was frequent, especially during winter, while a few cases of inorganic N limitation were observed in summer. Thus, the question of the nutrient control in Alfacs remains still unanswered.

Our hypothesis is that phytoplankton production experiences a colimitation of nitrogen and phosphorus, and that the most limiting nutrient changes during the year, depending on the variability of the sources and sinks of both nutrients. Therefore, the general aim of this work is to ascertain, by means of an ecosystem model, which nutrient or nutrients potentially limit phytoplankton production in Alfacs and to describe the main sources and sinks of these nutrients and how they affect the phytoplankton community composition. In particular, we will test two main hypotheses. 1) nitrogen or phosphorus are most limiting for phytoplankton growth in different seasons affecting the plankton community composition. 2) this alternation can be explained by two processes that affect phosphorus availability, in addition to freshwater inputs: a) phosphorus release from the sediment after resuspension events due to wind stirring (Vidal, 1994); b) availability of dissolved organic phosphorus (DOP) as a source of P to phytoplankton through two non-exclusive mechanisms: remineralization to dissolved inorganic phosphorus (DIP) and direct uptake. Although the direct uptake of DOP has been shown by several experimental studies (Johannes, 1964; Currie and Kalff, 1984; Bentzen et al., 1992; Huang and Hong, 1999; Oh et al., 2002; Yamamoto et al., 2004) it is only rarely taken into account by ecological models. The input of detrital particulate phosphorus (PP) from freshwater could be another source of phosphorus (Aminot et al., 1993; Ruttenberg, 2001; Némery and Garnier, 2007). Although samples of particulate matter in the channels are very scarce, the few available data suggest that the concentration of particulate phosphorus (PP) ranges between 1 and 3 mmol P m^{-3} (Muñoz, 1998). We did not present this third possibility in this manuscript because the fluxes of PP to the bay and the dissolution rates seem too small to add any substantial source of phosphorus to the bay.

In order to approximate the budgets and fluxes of nitrogen and phosphorus and to address the above hypotheses, we built a zero-dimensional ecological model of the estuarine mixed layer. The model includes nine state variables: zooplankton, flagellates, diatoms, dissolved inorganic nitrogen, dissolved inorganic phosphorus, dissolved organic nitrogen, dissolved organic phosphorus, detrital phosphorus, and detrital nitrogen. The forcing variables are water density, temperature, wind intensity, freshwater input, and velocities in and out of the bay, in addition to silicon that is introduced into the model based on a time series of measured concentrations.

In Section 2 we present the model equations and parameter values, and the choice of initial conditions and forcing used in the simulations. We also describe the field data. Section 3 reports the outcome of the various simulations using different sets of assumptions about the occurrence of sediment resuspension and the possibility of DOP utilization by phytoplankton, and presents the comparisons of these results with measured data. Section 4 presents a sensitivity analysis with respect to the fluxes and nutrient concentrations of the freshwater sources. The results are discussed in Section 5. Finally, we summarize our conclusions in Section 6.

2. Materials and methods

2.1. Study site

Alfacs Bay (Fig. 1) is the southernmost bay of the Ebre River deltaic complex (40°33′–40°38′N, 0°33–0°44′E), and also the largest. It is roughly 11 km long and 4 km wide; its average depth is 3.13 m and the maximum depth is 6.5 m; it contains approximately 153×10^6 m^3 of water. A sand barrier separates the basin from the sea. The mouth of the bay is about 2.5 km wide allowing water to be exchanged with the open sea along its eastern and southern periphery (Camp, 1994).

2.2. The model

The model used in this study is a zero dimensional mixed layer model that describes the nitrogen and phosphorus cycles of a shallow non-tidal estuarine bay. The temporal rate of change of any biochemical variable of the model (C) follows the equation,

$$\frac{\partial C}{\partial t} = G_{(C)}, \tag{1}$$

where $G_{(C)}$ represents the physical and biological sources minus sinks of the model variable.

The mixed layer deepening and shallowing are calculated using buoyancy and wind stress. The model considers horizontal advection due to exchanges with the open sea across the bay mouth, and to freshwater inputs from channels and underground seepage. Advection is included in the $G_{(C)}$ term. Horizontal diffusion is neglected because it is too small compared to advective transport to warrant inclusion in the model.

The dynamics of the state variables, Zooplankton (ZOO), Diatoms (PH1), Flagellates (PH2), Dissolved Inorganic Nitrogen (DIN), Dissolved Inorganic Phosphorus (DIP), Dissolved Organic Nitrogen (DON), Dissolved Organic Phosphorus (DOP), Detrital phosphorus (DTP) and Detrital nitrogen (DTN) are described by Eqs. (3) to (11) in Table 1. See Fig. 2 for a schematic diagram of the model and Table 2 for a description of the model parameters. The model is forced by six variables: water density, wind, rainfall, temperature, sea exchange, and freshwater inputs, which include discharge from channels and underground waters (Fig. 3, Table 3).

2.2.1. Physical processes

The model includes an approximation of the basic physical processes in Alfacs, which include a calculation of the mixed layer depth, and advection.

2.2.1.1. Mixed layer depth. The mixed layer depth represents the depth range through which the upper water column has been mixed in the recent past. It can be defined by a difference in temperature or density from the surface water, or by a gradient in temperature or density (Brainerd and Cregg, 1995). Because of the scarcity of data, we only have climatological temperature and salinity at two different depths of Alfacs. Therefore, we estimated the mixed layer depth based upon the Richardson Number and stratification relationship defined by Fisher et al. (1979). The Richardson Number indicates the potential mixing of an estuary and can be calculated as the ratio between the buoyancy due to differences of density and the kinetic energy due to the wind. Fisher et al. (1979) define four regimes (A, B, C, and D) that range from weak wind forcing and strong stratification (regime A) to strong wind forcing, causing a well mixed column (regime D). The range of winds and water densities in Alfacs suggests a transition between regime B and C when the wind is stronger than 5 m/s (Llebot, 2007). Regime B is characterized by internal waves and a sharp thermocline, while regime C has a mixed water column. The transition between regime B and C is defined by Fisher et al. (1979) to be at $Ri = (L/2h)^2$, where L is the length scale of the bay, and h is the mixed layer depth. By substituting this value into the Richardson Number expression,

$$Ri = \frac{\Delta\rho g h}{\rho_0 u^{*2}} \tag{2}$$

Table 1
Governing equations.

$$\frac{\partial PH1}{\partial t} = Growth_{(PH1)}PH1 - Death_{(PH1)}PH1 - Exudation_{(PH1)}PH1 - Grazing_{(PH1)}ZOO + Advection_{(PH1)} \tag{3}$$

$$\frac{\partial PH2}{\partial t} = Growth_{(PH2)}PH2 - Death_{(PH2)}PH2 - Exudation_{(PH2)}PH2 - Grazing_{(PH2)}ZOO + Advection_{(PH2)} \tag{4}$$

$$\frac{\partial ZOO}{\partial t} = \gamma(Grazing_{(PH2)} + Grazing_{(PH1)})ZOO - Death_{(ZOO)}ZOO^2 - Excretion_{(ZOO)}ZOO - Exudation_{(ZOO)}ZOO + Advection_{(ZOO)} \tag{5}$$

$$\frac{\partial DIN}{\partial t} = -Growth_{(PH2)}PH2 - Growth_{(PH1)}PH1 + Excretion_{(ZOO)}ZOO + Remineralization_{(DONtoDIN)}DON + FWInput_{(DIN)} + Advection_{(DIN)} \tag{6}$$

$$\frac{\partial DIP}{\partial t} = (R_{NP})^{-1}(-Growth\_eq_{(PH2)}PH2 - Growth\_eq_{(PH1)}PH1 + Excretion_{(ZOO)}ZOO) + XRemineralization_{(DOPtoDIP)}\,a\,DOP + FWInput_{(DIP)} + Resuspension_{(DIP)} + Advection_{(DIP)} \tag{7}$$

$$\frac{\partial DTN}{\partial t} = (1-\gamma)(Grazing_{(PH2)} + Grazing_{(PH1)})ZOO + Death_{(PH2)}PH2 + Death_{(PH1)}PH1 + Death_{(ZOO)}ZOO^2 - Remineralization_{(DTNtoDON)}DTN + Sedimentation_{(DTN)} + Advection_{(DIN)} + \tag{8}$$

$$\frac{\partial DTP}{\partial t} = (R_{NP})^{-1} \times ((1-\gamma) \times (Grazing_{(PH2)} + Grazing_{(PH1)})ZOO + Death_{(PH2)}PH2 + Death_{(PH1)}PH1 - Death_{(ZOO)}ZOO^2) - Remineralization_{(DTPtoDOP)}DTP + Sedimentation_{(DTP)} + Advection_{(DIN)} \tag{9}$$

$$\frac{\partial DOP}{\partial t} = (R_{NP})^{-1}(Exudation_{(PH1)}PH1 + Exudation_{(PH2)}PH2 + Exudation_{(ZOO)}ZOO - (Growth_{(PH2)} - Growth\_eq_{(PH2)})PH2 - (Growth_{(PH1)} - Growth\_eq_{(PH1)})PH1) + FWInput_{(DOP)} + Remineralization_{(DTPtoDOP)}DTP - Remineralization_{(DOPtoDIP)}\,a\,DOP + Advection_{(DOP)} \tag{10}$$

$$\frac{\partial DON}{\partial t} = Exudation_{(PH1)}PH1 + Exudation_{(PH2)}PH2 + Exudation_{(ZOO)}ZOO - Remineralization_{(DONtoDIN)} + Remineralization_{(DTNtoDON)} + Advection_{(DON)} \tag{11}$$

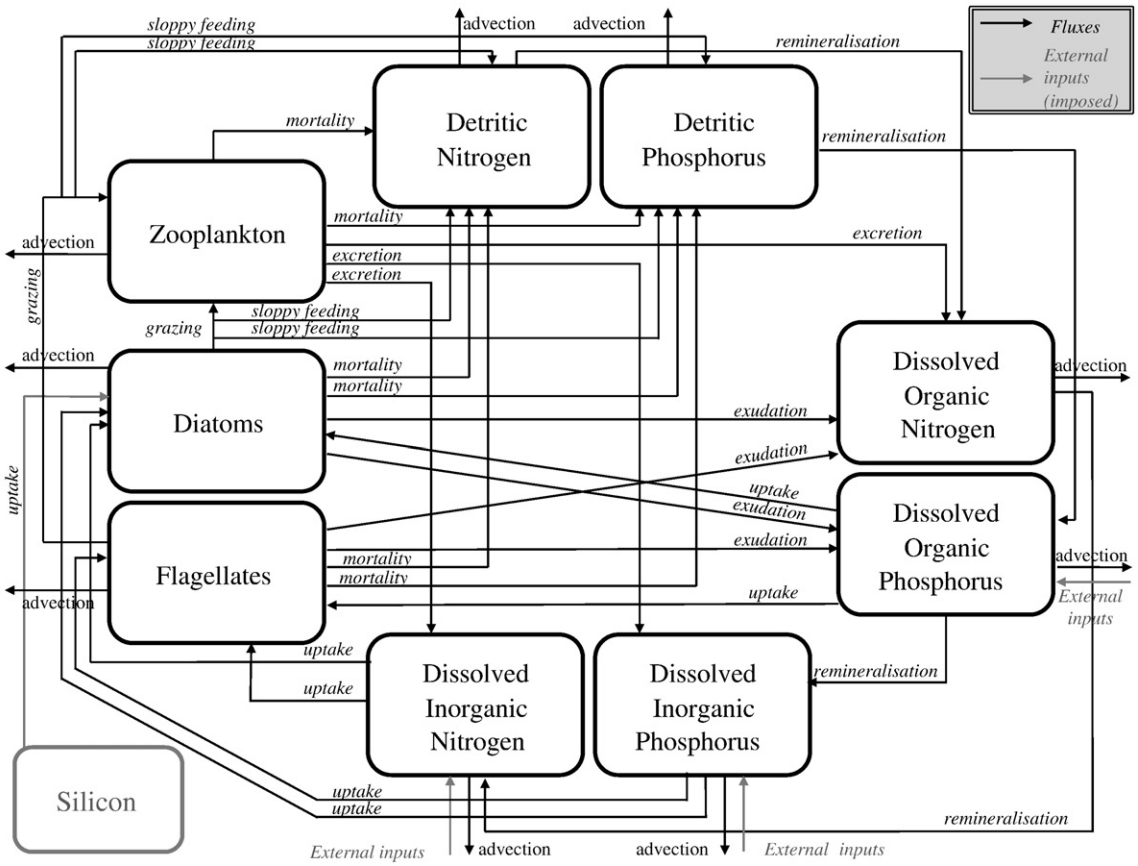

Fig. 2. Diagram of the model fluxes and state variables.

$\Delta\rho$ being the difference in water density between bottom and surface layers, g acceleration of gravity, ρ_0 a reference density, and u^* surface shear velocity, we obtained Eq. (32) (Table 4), with which we calculated an approximation of the mixed layer depth for the model runs. Results were smoothed with a 48 h filter (Fig. 3).

2.2.1.2. Advection terms. Fluxes across the mouth of the bay are called Advection in the equations of Table 1. Advection represents the flux in and out of the bay for the mixed layer and was calculated using a hydrodynamical three dimensional model. The model, referred to as Semi-Implicit Three-Dimensional Model for Estuarine Circulation (Si3D) (Smith, 2006), is a free-surface, hydrostatic, primitive equation model that has been used in studies of lacustrine systems (Rueda et al., 2003a,b; Rueda and Cowen, 2005) and currently implemented for Alfacs (Llebot et al., 2009). The model is forced by tide, atmospheric forcing, and freshwater inputs; these inputs are included in a similar fashion as in the present study.

In order to calculate the advective transport of the model variables, the Si3D velocity field was first averaged over the basin and then rotated in the direction parallel to the coast and perpendicular to the mouth of the bay. By using a principal component analysis of currents at the center of the bay, Artigas (2008) showed that the dominant current directions are parallel to the coast (East direction -15°) and perpendicular to the coast (North direction -15°). The calculation of Advection with Eqs. (25), (26) and (27) (Table 4) is performed using the component of the current velocity that corresponds to the East–West direction minus 15°. The results are shown in Fig. 3. Advection of the various concentrations is computed assuming that the sea concentrations are the ones in the bay recorded the previous day and multiplied by a dilution factor of 72%, which reflects a residence time of 5 to 12 days of the Alfacs waters on the Ebre shelf (Salat et al., 2002).

Freshwater inputs (FWInput) enter the bay by two different means: discharge channels from rice fields and underground water seepage. We assume that the only non-negligible scalars carried by freshwater are nitrogen and phosphorus, in organic and inorganic forms. Freshwater sources from water treatment plants have not been included, because they only represent roughly 0.01% of the land inputs (Camp, 1994). See Section 2.3 for information about the fluxes and Eq. (29) (Table 4) for details about their computation.

2.2.2. Biogeochemical processes

The growth of flagellates and diatoms is controlled by nutrients, light, and temperature. In addition to DIN and DIP, nutrients include Dissolved Organic Phosphorus (DOP) and silicon (Si) (for diatom growth). Si is imposed in the model based on monthly averages of observations carried out between April 2007 and March 2008 (Loureiro et al., 2009). Both groups of phytoplankton are grazed by one generic group of zooplankton. Dead phytoplankton cells go to the detritus pool, as do dead zooplankton, and the fraction of grazed phytoplankton that is not assimilated. Detritus pools have a loss by sinking and are metabolized to organic nitrogen and phosphorus, which also receive inputs from phytoplankton exudation. Organic nutrients are remineralized to inorganic nitrogen and phosphorus. Zooplankton excrete nitrogen and phosphorus to both the organic and inorganic pools.

2.2.2.1. Growth. Phytoplankton growth in this model is controlled by light, temperature, and nutrients (Eqs. (12) and (13), Table 4). The maximum growth rates were initially chosen following Merico et al. (2004), and further adapted by means of recursive simulations, keeping the values within the usual ranges for ecological models (van den Berg et al., 1995; Lacroix and Nival, 1998; Chapelle et al., 2000; Lima et al., 2002; le Quéré et al., 2005; Giraud, 2006; Kishi et al., 2007).

Table 2
Parameters.

Symbol	Value	Units	Description
Basic parameters of the model			
dt	15	min	Time step
Basic parameters of the plankton			
$P^{\beta}_{m(\mathrm{PH1})}$	1.45	day^{-1}	Maximum diatom growth rate
$P^{\beta}_{m(\mathrm{PH2})}$	1.0	day^{-1}	Maximum flagellate growth rate
$Kp_{(\mathrm{PH1})}$	0.8	$\mathrm{mmol\ N\ m}^{-3}$	Diatom half saturation constant for zooplankton ingestion
$Kp_{(\mathrm{PH2})}$	0.8	$\mathrm{mmol\ N\ m}^{-3}$	Flagellate half saturation constant for zooplankton ingestion
$m_{(\mathrm{PH1})}$	0.15	day^{-1}	Diatom mortality rate
$m_{(\mathrm{PH2})}$	0.15	day^{-1}	Flagellate mortality rate
$m_{(\mathrm{ZOO})}$	0.08	day^{-1}	Zooplankton mortality rate
R_m	1	day^{-1}	Zooplankton maximum grazing rate
$\chi_{(\mathrm{PH1})}$	0.2	No dim	Preference of zooplankton for grazing on diatom
$\chi_{(\mathrm{PH2})}$	0.8	No dim	Preference of zooplankton for grazing on flagellate
$Q_{(\mathrm{PH1})}$	0.04	day^{-1}	Diatom exudation rate
$Q_{(\mathrm{PH2})}$	0.04	day^{-1}	Flagellate exudation rate
$Q_{(\mathrm{ZOO})}$	0.05	day^{-1}	Zooplankton excretion rate to DON and DOP
E	0.03	day^{-1}	Zooplankton excretion rate to DTN and DTP
R_{NP}	16	mol/mol	Redfield ratio
Basic parameters of the bay			
A	49,000,000	m^2	Area
ML	2500	m	Mouth length
ϕ	40.5	°N	Latitude
Light limitation			
PAR	0.48	%	Photosynthetically active radiation
I_0	340	$\mathrm{W\ m}^{-2}$	Incoming solar radiation
θ	0.04	No dim	Albedo
$\alpha_{(\mathrm{PHX})}$	0.1	$\mathrm{mmol\ N\ h}^{-1}\ \mathrm{W}^{-1}\ \mathrm{m}^{-2}$	Slope of the light saturation curve
Temperature limitation			
$T_{opt(PHU)}$	16	°C	Optimal growth temperature for diatoms
$T_{opt(PHD)}$	17	°C	Optimal growth temperature for flagellates
$dT_{(PHU)}$	12	°C	Optimal temperature interval for diatoms
$dT_{(PHD)}$	15	°C	Optimal temperature interval for flagellates
Colimitation of nutrients			
$Ks_{(\mathrm{DIN,\ PH1})}$	0.8	$\mathrm{mmol\ N\ m}^{-3}$	DIN half saturation constant for diatoms
$Ks_{(\mathrm{DIP,\ PH1})}$	0.085	$\mathrm{mmol\ P\ m}^{-3}$	DIP half saturation constant for diatoms
$Ks_{(\mathrm{P,\ PH1})}$	0.085	$\mathrm{mmol\ P\ m}^{-3}$	P half saturation constant for diatoms
$Ks_{(\mathrm{DOP,\ PH1})}$	0.085	$\mathrm{mmol\ P\ m}^{-3}$	DOP half saturation constant for diatoms
$Ks_{(\mathrm{Si,\ PH1})}$	1	$\mathrm{mmol\ Si\ m}^{-3}$	Si half saturation constant for diatoms
$Ks_{(\mathrm{DIN,\ PH2})}$	0.65	$\mathrm{mmol\ N\ m}^{-3}$	DIN half saturation constant for flagellates
$Ks_{(\mathrm{DIP,\ PH2})}$	0.04	$\mathrm{mmol\ P\ m}^{-3}$	DIP half saturation constant for flagellates
$Ks_{(\mathrm{P,\ PH2})}$	0.04	$\mathrm{mmol\ P\ m}^{-3}$	P half saturation constant for flagellates
$Ks_{(\mathrm{DOP,\ PH2})}$	0.04	$\mathrm{mmol\ P\ m}^{-3}$	DOP half saturation constant for flagellates
$a_{(\mathrm{DON})}$	0.1	No dim	Fraction of bioavailable DON
$a_{(\mathrm{DOP})}$	0.5	No dim	Fraction of bioavailable DOP
Sedimentation			
$\varphi_{(\mathrm{DTN})}$	10	$\mathrm{m\ s}^{-1}$	Sinking velocity of DTN
$\varphi_{(\mathrm{DTP})}$	10	$\mathrm{m\ s}^{-1}$	Sinking velocity of DTP
Mixed layer depth			
L	11,000	m	Length scale of the bay
g	9.81	$\mathrm{m\ s}^{-2}$	Acceleration of gravity
C_D	1.3×10^{-3}	No dim	Drag coefficient
ρ_a	1.2	$\mathrm{kg\ m}^{-3}$	Air density
Inputs of freshwater			
$C_{(dis,\ \mathrm{DIN})}$	35	$\mathrm{mmol\ N\ m}^{-3}$	Concentration of DIN in discharge channels
$C_{(dis,\ \mathrm{DIP})}$	0.5	$\mathrm{mmol\ P\ m}^{-3}$	Concentration of DIP in discharge channels
$C_{(dis,\ \mathrm{DOP})}$	5	$\mathrm{mmol\ P\ m}^{-3}$	Concentration of DOP in discharge channels during the months of rice cultivation (April to July)
$C_{(dis,\ \mathrm{DOP})}$	3	$\mathrm{mmol\ P\ m}^{-3}$	Concentration of DOP in discharge channels during fallow months (August to March)
$C_{(dis,\ \mathrm{DON})}$	25	$\mathrm{mmol\ N\ m}^{-3}$	Concentration of DON in discharge channels
$C_{(und,\ \mathrm{DIN})}$	300	$\mathrm{mmol\ N\ m}^{-3}$	Concentration of DIN in underground water
$C_{(und,\ \mathrm{DIP})}$	0.5	$\mathrm{mmol\ P\ m}^{-3}$	Concentration of DIP in underground water
$C_{(und,\ \mathrm{DOP})}$	0	$\mathrm{mmol\ P\ m}^{-3}$	Concentration of DOP in underground water
$C_{(und,\ \mathrm{DON})}$	0	$\mathrm{mmol\ N\ m}^{-3}$	Concentration of DON in underground water
F_{und}	60,480	$\mathrm{m}^3\ \mathrm{day}^{-1}$	Underground water flow
Resuspension of sediments			
$Pflow$	30	$\mathrm{mmol\ m}^{-2}\ \mathrm{h}^{-1}$	Mean DIP flow for the first 30 min after the sediment resuspension.
Peq	0.2	$\mathrm{mmol\ m}^{-3}$	Equilibrium concentration of DIP after 30 min from the sediment resuspension

Table 2 (*continued*)

Symbol	Value	Units	Description
Advection			
Dilution	72	$\%\,day^{-1}$	Dilution rate
Remineralization			
$D_{DTNtoDON}$	0.1	day^{-1}	Detritic nitrogen remineralization rate to DON
$D_{DTPtoDOP}$	0.2	day^{-1}	Detritic phosphorus remineralization rate to DOP
$D_{DONtoDIN}$	0.1	day^{-1}	DON remineralization rate to DIN
$D_{DOPtoDIP}$	0.1	day^{-1}	DOP remineralization rate to DIP

The maximum growth rate for diatoms is higher than the maximum growth rate for flagellates, as in Kishi et al. (2007), Lacroix and Nival (1998) or Merico et al. (2004).

Many mathematical expressions have been proposed to relate primary productivity to irradiance (I). Most of them (e.g., Jassby and Platt, 1976; Platt et al., 1980) use two common parameters: the slope of the light-saturation curve at low light levels (α), and the maximum specific photosynthetic rate (P_m^B). As the curves obtained are very similar, we chose one of the simplest equations (Table 4, Eq. (15)), from Smith (1936). The variable I in Eq. (15) (Table 4) is the irradiance received by the cell and is calculated from Eq. (16) (Table 4), which uses the incoming solar radiation I_0, the percentage of Photosynthetically Active Radiation (PAR), albedo (θ), and day length (Matlab program from Fennel and Neumann (2004)). As our model is only considering the mixed layer, which is very shallow (less than 6 m deep), depth dependence was not taken in account. The photosynthetic parameters (Table 2) of Eq. (16) (Table 4) are taken from Fennel et al. (2002).

Phytoplankton growth is controlled by temperature following Eq. (17) (Table 4) (Lancelot et al., 2005). It is an exponential temperature dependence on the optimal growth temperature (T_{opt}) and a temperature interval (dT). Temperature dependence has not been set for the other biological processes because uncertainties in its parameterization added complexity, rather than insight, to the model. All the parameters of the model in Table 2 have been established according to the range of temperatures (10–28 °C, Fig. 3) observed in the bay.

Nutrient uptake is parameterized using a colimitation equation (Lancelot et al., 2005), which has been shown to represent accurately the observations in the case of multiple nutrient limitations (O'Neill et al., 1989). Diatoms are limited by nitrogen, phosphorus, and silicon (Table 4, Eq. (20)), while flagellates are only limited by nitrogen and phosphorus (Table 4, Eq. (21)).

Phytoplankton and bacteria can use some organic P substrates by the action of phosphomonoesterase enzymes. The most widely recognized of these enzymes in aquatic systems is the alkaline phosphatase (Bentzen et al., 1992). Particularly in situations of phosphorus stress, phytoplankton have a notable capacity for phosphorus uptake from organic sources (Currie and Kalff, 1984). Therefore, DOP is considered as a state variable and DOP uptake is taken into account in the model. The origin of DOP can be excretion from living microbes, plants and animals, or decomposition from dead organisms. Therefore, a large proportion of the DOP is formed by high molecular weight or colloidal material that is not readily available for uptake. The bioavailability fraction taken in the model ($a_{(DOP)}$ in Table 2) is similar to the values found in Huang and Hong (1999). In the colimitation equation used for the calculation of the nutrient uptake (Table 4, Eq. (18)), phosphorus is entered as the sum of DIP and the bioavailable fraction of DOP (Table 4, Eqs. (20) and (21)), and a common half saturation constant for all phosphorus pools is used (Table 2). In order to calculate the proportion of phosphorus used from the DIP pool (named $Growth\_eq_{(PHX)}$ in Table 1) and from the DOP pool, we use Eq. (14) (Table 1), following Spitz et al. (2001). We have utilized this formulation instead of a ratio of the DIP and DOP concentrations since we assume an energetic approach to phytoplankton growth. The amount of DIP required for growth is first calculated, and if more phosphorus is required then DOP uptake is allowed. Thus, Eq. (14) (Table 1) gives preference to DIP uptake over DOP uptake.

The half saturation constants for DIN uptake are taken from the range found in the literature (Lacroix and Nival, 1998; Fennel et al., 2002; Lima et al., 2002). The half saturation constant for flagellates is set lower, meaning that this group has a higher affinity for the substrate, as in Crispi et al. (2002), Lacroix and Nival (1998), and Merico et al. (2004). The half saturation constant for DIP uptake is taken from Tyrrell (1999), and modified according to the range measured by Taft et al. (1975). The half saturation constant for silicon uptake is taken from van den Berg et al. (1995) and slightly modified for better agreement with observations. The half saturation constant for DOP uptake is within the ranges measured in Bentzen et al. (1992) for bacteria and is similar to the values used in other models including DOP (Chen et al., 2002).

2.2.2.2. Zooplankton grazing. As Franks (2002) states in his review of NPZ models, representation of zooplankton grazing has always presented a complex problem. The formulation can include a saturating response to increasing food, grazing thresholds, varying degrees of nonlinearity and acclimation of the grazing rate to changing food conditions. We used a saturating formulation with preferences of grazing as in Fasham et al. (1990) (see Eqs. (23) and (24), Table 4).

2.2.2.3. Other formulations. Mortality of both zooplankton and phytoplankton is expressed following a linear parameterization with a constant mortality rate m (Table 4 Eq. (38)). This rate was taken from the same literature as the phytoplankton growth rate, but in addition it includes a component that corresponds to filtering by mussels, which are cultured in about 90 rafts in the northern half of the bay. *Excretion*, *Exudation* and *Remineralization* are parameterized linearly with constant rates E (Table 4, Eq. (39)), Q (Table 4, Eq. (42)) and D (Table 4, Eq. (41)) respectively. The values of these rates are obtained from Crispi et al. (2002) and Pinazo et al. (1996). Detrital *Sedimentation* is expressed with a constant sinking velocity using Eq. (34) (Table 4). The effect of metabolic pathways such as denitrification (Mallo et al., 1993) is assumed to be included in the parameterization of the remineralization process.

2.3. Forcing variables

See Table 3 for a summary of the forcing variables, and Fig. 3 for graphs of the data. *Density* and *Temperature* are taken from a climatology based on 14 years of field data (de Pedro, 2007; Solé et al., 2009). *Silicon* is obtained from Loureiro et al. (2009). They calculated monthly averages based on weekly samples taken between April 2007 and March 2008, from surface water (0.5 m depth) at a station located in the center of Alfacs Bay (40° 36′ 0″N, 0° 39′ 0″E). An annual composition of these data is shown in Fig. 3. *Wind speed and direction* are obtained from an automatic weather station (named Els Alfacs) managed by the Meteorological Service of Catalonia (SMC) located on

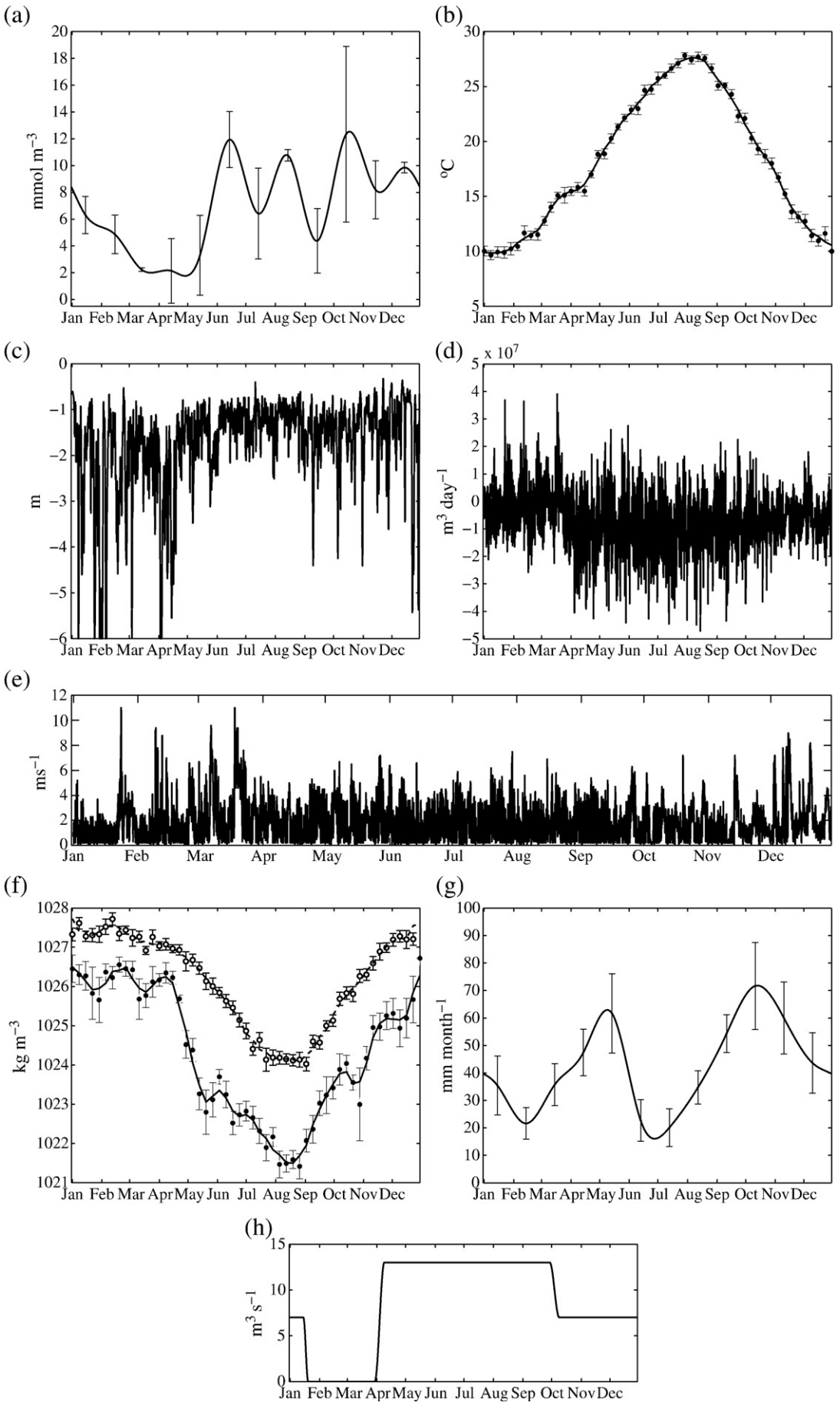
(a)
mmol m^{-3}
(b)
ºC
(c)
m
(d)
x 10^7
m^3 day^{-1}
(e)
ms^{-1}
(f)
kg m^{-3}
(g)
mm month^{-1}
(h)
m^3 s^{-1}
Jan Feb Mar Apr May Jun Jul Aug Sep Oct Nov Dec

Table 3
Forcing variables. See Fig. 3 for details.

Symbol	Units	Description	Value
Si	mmol Si m^{-3}	Silicon concentration	Loureiro et al. (2009)
DOP	mmol P m^{-3}	Dissolved organic phosphorus	Loureiro et al. (2009)
R	mm $month^{-1}$	Monthly accumulated rainfall	National Institute of Meteorology
u	m s^{-1}	Wind speed	Wind measured at an automatic meteorological station 2007
$F_{(dis)}$	m^3 day^{-1}	Discharge channel flow	Literature (see Section 2.3)
ρ	kg m^{-3}	Water density	Calculated from T and salinity climatologies
T	°C	Water temperature	T climatology
V_0	m/s	Velocity of water in and out the bay	Physical model Si3D

the north shelf of the bay (40° 37′N, 0° 40′E; see Fig. 1). Monthly accumulated *rainfall* climatology is calculated using daily data from the National Institute of Meteorology. The station, Roquetes (Tortosa), is located 10 km north from the bay, next to the Ebro River, and the data set covers a period from 1990 to 2004. A cubic spline interpolation was performed to fit the data set to the time step used in the model.

Forcing by freshwater inflow includes *discharge channel flux* and *underground water inputs*. Freshwater enters Alfacs Bay from a network of controlled drainage channels coming from the rice fields. Rice is cultivated on 57% of the surface of the Ebre Delta (about 7880 Ha), in lands flooded to a depth of 15–20 cm (Farnós et al., 2007). The growing season lasts approximately 190 days, from the beginning of April to the end of September. Rice is planted as a seed a week after flooding, which is followed by a vegetative period (95 days), a reproductive period (20 days) and a ripening period (40 days) (Forès and Comín, 1992). During these periods the freshwater flux to the bays is maximum (1.84×10^{-3} m^3 s^{-1} ha^{-1}). Since 2001, a lower flux from the channels (1×10^{-3} m^3 s^{-1} ha^{-1}) is maintained after the crop for agroenvironmental reasons. This situation lasts about 120 days, from October to mid January. Finally, from mid January to the end of March, the channels are closed, and the discharge channel flux is 0. When the water starts flowing again, all the fields are flooded with 15 cm of water in 10 days. The temporal evolution of the channel freshwater discharge during the year is shown in Fig. 3.

Nutrient concentrations in the waters entering the bay are one of the most important forcing factors that need to be specified in the model. Given the high variability of the nitrogen concentration in the channels (see Table 5) and the lack of data to assess its potential temporal dependence, a constant value of 35 mmol N m^{-3} is adopted for DIN. The concentration of DON has been set to 25 mmol N m^{-3} because, although we do not have measurements, there is evidence that the value is of the same order as DIN (Forès, 1992). The case for phosphorus is similar (Table 5), but even less data are available. A constant value of 0.5 mmol P m^{-3} is chosen as the DIP concentration in the freshwater input. There are no direct measurements of DOP concentration in the channels. However, there is evidence that the rice field release higher DOP concentrations during the first stages of the crop (Muñoz, 1998). Therefore, a high value of DOP concentration in the channels (5 mmol P m^{-3}) is chosen from April to August, and a lower concentration (3 mmol P m^{-3}) from September to March. These values are within the range found in other rivers and estuaries (Hernández et al., 2000; Monbet et al., 2009). The DOP concentrations predicted with these inflows will be compared with measured DOP values within Alfacs.

Table 4
Equations.

Growth:

$$\mathrm{Growth}_{(\mathrm{PH1})} = \mathrm{Uptake}_{(\mathrm{PH1})}\mathrm{LightLim}_{(\mathrm{PH1})}\mathrm{TempLim}_{(\mathrm{PH1})} \quad (12)$$

$$\mathrm{Growth}_{(\mathrm{PH2})} = \mathrm{Uptake}_{(\mathrm{PH2})}\mathrm{LightLim}_{(\mathrm{PH2})}\mathrm{TempLim}_{(\mathrm{PH2})} \quad (13)$$

$$\mathrm{Growth\_eq}_{(\mathrm{PHX})} = \mathrm{Growth}_{(\mathrm{PHX})} - \mathrm{Growth}_{(\mathrm{PHX})}\frac{\mathrm{Upt}_{(\mathrm{DOP,PHX})}}{\mathrm{Upt}_{(\mathrm{DOP,PHX})} + \mathrm{Upt}_{(\mathrm{DIP,PHX})}} \quad (14)$$

Light limitation:

$$\mathrm{LightLim}_{(\mathrm{PHX})} = \frac{P^B_{m(\mathrm{PHX})}\alpha_{(\mathrm{PHX})}I}{\sqrt{(P^B_{m(\mathrm{PHX})})^2 + \alpha^2_{(\mathrm{PHX})}I^2}} \quad (15)$$

$$I = PARI_0(1-\theta)\mathrm{DayLength} \quad (16)$$

Temperature limitation:

$$\mathrm{TempLim}_{(\mathrm{PHX})} = \exp\left[\frac{((T-T_{opt(\mathrm{PHX})})^2}{dT^2_{(\mathrm{PHX})}}\right] \quad (17)$$

Nutrient limitation:

$$\mathrm{P} = \mathrm{DIP} + a_{(\mathrm{DOP})}\mathrm{DOP} \quad (18)$$

$$\mathrm{Uptake}_{(\mathrm{PH1})} = \frac{1}{1 + \frac{Ks_{(\mathrm{Si,PH1})}}{\mathrm{Si}} + \frac{Ks_{(\mathrm{DIN,PH1})}}{\mathrm{DIN}} + \frac{Ks_{(\mathrm{P,PH1})}}{\mathrm{P}}} = \frac{\mathrm{SiDINP}}{\mathrm{SiDINP} + Ks_{(\mathrm{Si,PH1})}\,\mathrm{DINP} + Ks_{(\mathrm{DIN,PH1})}\,\mathrm{SiP} + Ks_{(\mathrm{P,PH1})}\,\mathrm{DINSi}} \quad (19)$$

$$\mathrm{Uptake}_{(\mathrm{PH2})} = \frac{1}{1 + \frac{Ks_{(\mathrm{DIN,PH2})}}{\mathrm{DIN}} + \frac{Ks_{(\mathrm{P,PH2})}}{\mathrm{P}}} = \frac{\mathrm{DINP}}{\mathrm{DINP} + Ks_{(\mathrm{DIN,PH2})}\,\mathrm{P} + Ks_{(\mathrm{P,PH2})}\,\mathrm{DIN}} \quad (20)$$

$$\mathrm{Upt}_{(\mathrm{DIP,PHX})} = \frac{\mathrm{DIP}}{Ks_{(\mathrm{DIP,PHX})} + \mathrm{DIP}} \quad (21)$$

$$\mathrm{Upt}_{(\mathrm{DOP,PHX})} = (1-\mathrm{Upt}_{(\mathrm{DIP,PHX})})\frac{a_{(\mathrm{DOP})}\,\mathrm{DOP}}{Ks_{(\mathrm{DOP,PHX})} + a_{(\mathrm{DOP})}\,\mathrm{DOP}} \quad (22)$$

Grazing:

$$\mathrm{Grazing}_{(\mathrm{PH1})} = \frac{R_m\chi_{(\mathrm{PH1})}\mathrm{PH1}^2}{Kp_{(\mathrm{PH1})}(\chi_{(\mathrm{PH2})}\mathrm{PH2} + \chi_{(\mathrm{PH1})}\mathrm{PH1}) + \chi_{(\mathrm{PH2})}\mathrm{PH2}^2 + \chi_{(\mathrm{PH1})}\mathrm{PH1}^2} \quad (23)$$

$$\mathrm{Grazing}_{(\mathrm{PH2})} = \frac{R_m\chi_{(\mathrm{PH2})}\mathrm{PH2}^2}{Kp_{(\mathrm{PH2})}(\chi_{(\mathrm{PH2})}\mathrm{PH2} + \chi_{(\mathrm{PH1})}\mathrm{PH1}) + \chi_{(\mathrm{PH2})}\mathrm{PH2}^2 + \chi_{(\mathrm{PH1})}\mathrm{PH1}^2} \quad (24)$$

Advection:

$$\mathrm{Advection}_{(\mathrm{XXX})} = \frac{V_0 ML}{A}\Delta Conc_{(\mathrm{XXX})} \quad (25)$$

$$\mathrm{If}\ V_0>0 \quad \Delta Conc_{(\mathrm{XXX})} = \mathrm{XXX}_{(t-1\mathrm{day})}\,dilution - \mathrm{XXX} \quad (26)$$

$$\mathrm{If}\ V_0<0 \quad \Delta Conc_{(\mathrm{XXX})} = \mathrm{XXX} - \mathrm{XXX}_{(t-1\mathrm{day})}\,dilution \quad (27)$$

Inputs of freshwater:

$$\mathrm{FWInput}_{(\mathrm{DIX})} = \frac{F_{(dis)}C_{(dis,\mathrm{DIX})} + rF_{(und)}C_{(und,\mathrm{DIX})}}{AMLD} \quad (28)$$

$$r = rain + evaporation \quad (29)$$

(continued on next page)

Fig. 3. Imposed variables and forcing parameters. (a) Silicon (Redrawn from Loureiro et al. (2009)). (b) Climatological temperature at 0.5 m over the period 1990–2003 (○ weekly average. — three point average of the weekly averages). (c) Mixed layer depth. See text for details about the calculation. (d) Advective flow to (+) and from (−) the bay. (e) Wind speed. (f) Climatological density at 0.5 m (black) and 5.5 m (gray) over the period 1990–2003 (○ weekly average. — three point average of the weekly averages). (g) Rainfall climatology. Vertical bars indicate standard deviation. (h) Flux from discharge channels.

Table 4 (*continued*)

Inputs of freshwater:

$$rain = \frac{R - min(R)}{max(R) - min(R)} + 1 \quad (30)$$

$$evaporation = \frac{min(T)}{T} \quad (31)$$

Mixed layer depth:

$$MLD = \sqrt{\frac{\rho L}{2\Delta\rho g} u^{*2}} \quad (32)$$

$$u^{*2} = C_D \frac{\rho_a}{\rho} u^2 \quad (33)$$

Sedimentation:

$$\text{Sedimentation}_{(DTX)} = -\frac{\partial}{\partial z}\left((\phi_{(DTX)})DTX\right) \quad (34)$$

Resuspension of sediment:

$$\text{whenMLD(t)} = 6 \quad \text{Resuspension}_{(DIX,t)} = Pflow \quad (35)$$

$$\text{Resuspension}_{(DIX,t\ +\ 30min)} = Pflow \quad (36)$$

$$\text{Resuspension}_{(DIX,t\ +\ 31min)} = 0; DIP = Peq \quad (37)$$

Death:

$$\text{Death}_{(XXX)} = m_{(XXX)} \quad (38)$$

Excretion:

$$\text{Excretion}_{(ZOO)} = E \quad (39)$$

Remineralization:

$$\text{Remineralization}_{(DTXtoDOX)} = D_{(DTXtoDOX)} \quad (40)$$

$$\text{Remineralization}_{(DOXtoDIX)} = a_{(DOX)} D_{(DOXtoDIX)} \quad (41)$$

Exudation:

$$\text{Exudation}_{(XXX)} = Q_{(XXX)} \quad (42)$$

XXX means any variable, PHX any phytoplankton group, DIX any dissolved inorganic variable, DOX any dissolved organic variable, and DTX any detritus group.

The *underground inputs of freshwater* were suggested to be 0.7 $m^3\ s^{-1}$ by Camp (1994). However, recent modeling studies have shown that this value is probably underestimated (Llebot, 2007). Because of the lack of data we approximate the underground input of freshwater as follows. The baseline flow is fixed to 0.7 $m^3\ s^{-1}$, as suggested by Camp (1994). The flow is modulated by two additive factors ranging from 0 to 1, which represent the variations due to evaporation and rainfall (Boyle, 1994; Smith et al., 2008). It is assumed that the flow increases in the wet season and decreases with high temperature. In favorable conditions the flow almost doubles the baseline (as, for example, in Stalker et al. (2009)), while in dry and hot conditions it is close to zero.

Table 5
Measured concentrations of inorganic nutrients in the channels (mmol m^{-3}).

Reference	NH_3^-	NH_2^-	NH_4^+	PO_4^{3-}
Muñoz (1998)	20–80	2–14	10–100	
Camp and Delgado (1987)	15–45	1.6–2.8		0.8–1.5
de Pedro (2007) 1986–1987	29.8±7	3.34±1	19.3±5	1.0±0
de Pedro (2007) 1996–1997	85.3±16	6.35±2	76.1±29	0.6±0

Table 6
Initial conditions.

Symbol	Value	Units	Description
PH1	0.3	mmol N m^{-3}	First group of phytoplankton: diatoms
PH2	0.05	mmol N m^{-3}	Second group of phytoplankton: flagellates
ZOO	0.2	mmol N m^{-3}	Zooplankton
DIN	5.9	mmol N m^{-3}	Dissolved inorganic nitrogen
DIP	0.18	mmol P m^{-3}	Dissolved inorganic phosphorus
DTN	0.5	mmol N m^{-3}	Nitrogen fraction of the detritus
DTP	0.15	mmol P m^{-3}	Phosphorus fraction of the detritus
DON	0.1	mmol N m^{-3}	Dissolved organic nitrogen
DOP	0.1	mmol P m^{-3}	Dissolved organic phosphorus pool

There are very few observations of the concentration of nutrients in the underground water emptying into Alfacs Bay. Public records of underground water nitrate concentration at various locations in the area of the Ebre Delta (Agència Catalana de l'Aigua, available online), range from 20 mmol m^{-3} to 3000 mmol m^{-3}. We chose a value of 300 mmol m^{-3}, which is close to the mean. As we do not know the phosphate concentration in these waters, we assume that it is the same as in the freshwater channels (0.5 mmol P m^{-3}). Similar phosphate concentrations were found by Torrecilla et al. (2005) in underground waters in other parts of the Ebre River. We assumed that no organic nutrients in Alfacs originate from underground sources.

Theoretically, the adsorption/desorption reactions that take place in the sediment can have an important influence on the total concentration of dissolved inorganic phosphorus in the water column (Froelich, 1988; Lebo, 1991; Andrieux-Loyer and Aminot, 2001). Vidal (1994) studied the phosphate dynamics tied to sediment disturbances in Alfacs. She found a buffering effect that leads to a final concentration of about 0.2 to 0.3 mmol P m^{-3} of soluble reactive phosphorus (SRP) when the sediments are resuspended. However, if the sediments were not resuspended but just gently stirred, the SRP diffusion from the sediment was undetectable. In the model, we assumed that sediment resuspension occurs when the mixed layer depth reaches the bottom. In this case, there is a flow of phosphorus (DIP) from the sediment to the water column during the first 30 min. After this 30 min period, an equilibrium concentration is reached due to the buffering system described in Vidal (1994). The amount of phosphorus released during resuspension and the equilibrium concentration were fixed using the data in Vidal (1994) (see Table 2). Because no strong correlation between the release of certain organic compounds and oxygen uptake with temperature has been observed in Alfacs (Vidal et al., 1997), we have not taken into account the dependence of sediment PO_4 diffusion on temperature or oxygen.

The initial conditions for the model variables are taken from the January observations for dissolved inorganic nitrogen, dissolved inorganic phosphorus, dissolved organic nitrogen, dissolved organic phosphorus and diatoms. A first approximation is used for flagellates, detritus, and zooplankton. See Table 6 for the adopted values.

2.4. Design of the simulations

In order to explore the hypotheses, i.e., phosphorus and nitrogen limitation, importance of sediment resuspension and DOP, we

Table 7
Processes included in the five designed simulations.

Simulation name	Sediment resuspension	DOP input from channels	DOP uptake by phytoplankton
Standard Simulation	X	X	X
No Resuspension Simulation		X	X
No DOP Input Simulation	X		X
No DOP Uptake Simulation	X	X	
No Extra P Simulation			

designed several modeling experiments (Table 7). The first simulation incorporates DOP uptake for phytoplankton growth and resuspension of sediments (called *Standard Simulation* from now on). The second simulation includes DOP use but no sediment resuspension (*No Resuspension Simulation*). The third simulation comprises sediment resuspension but no DOP input from the channels (*No DOP Input Simulation*), although the option of DOP uptake by phytoplankton is still possible, since a DOP pool is formed by phytoplankton exudation, zooplankton excretion, and detrital remineralization. The fourth simulation includes sediment resuspension and DOP inputs, but not DOP uptake (*No DOP Uptake Simulation*). A fifth simulation with no DOP inputs from channels and no resuspension (*No Extra P Simulation*) has also been performed.

2.5. Observations

Weekly climatologies for temperature, salinity, and chlorophyll *a* were calculated from the data collected by the Aquaculture Center of IRTA (Institute for Food and Agricultural Research and Technology) from 1990 to 2003 and published by de Pedro (2007) and Solé et al. (2009). Additionally, nitrate concentrations (Fig. 4) were determined from 1991 to 1994 and phosphate concentrations from 1993 to 1994 (de Pedro, 2007). The water samples were collected weekly near the surface (0.5 m) at the center of the bay (Fig. 1). Phytoplankton from the same sampling site (M. Delgado, unpublished data) were counted by means of the Utermöhl technique, using 50 ml sedimentation chambers and a Nikon inverted microscope. Diatoms and dinoflagellates, as well as nano and microphytoplankton from other algal groups were identified down to the lowest possible taxonomical level and enumerated. A weekly climatology was calculated for diatoms, but not for flagellates, because the small size and poor conservation of many of these organisms make them unsuitable for the inverted microscope technique. This data set did not include measurements of organic nutrients. The data shown in Fig. 5 has been redrawn from Loureiro et al. (2009).

The diatom data, given in cell numbers per unit volume, were transformed to N units for comparison purposes. We used a conversion factor of 16.2 ± 1.8 pg N cell^{-1}, calculated by Segura (2007) for diatoms from the Catalan coast, using X ray microanalysis techniques (this factor represents averages of measurements for a number of cells and can vary depending on the species and on environmental characteristics). The modeled chlorophyll *a* of Fig. 6(e) was obtained by adding the N concentration of the two phytoplankton groups, using the Redfield ratio to calculate phytoplankton carbon and applying a carbon:chlorophyll ratio of 40 mg/mg, within the range reported by Arin et al. (2002).

Figs. 3–6 show the weekly means and the standard error of the mean of these physical, chemical, and biological data. A smoothing of the data was performed using the average of three consecutive averages.

3. Results

The observations and model results are shown in Figs. 4, 5 and 6. The *No Extra P Simulation* (no DOP inputs from channels and no resuspension) gave generally similar results to the *No DOP Input*

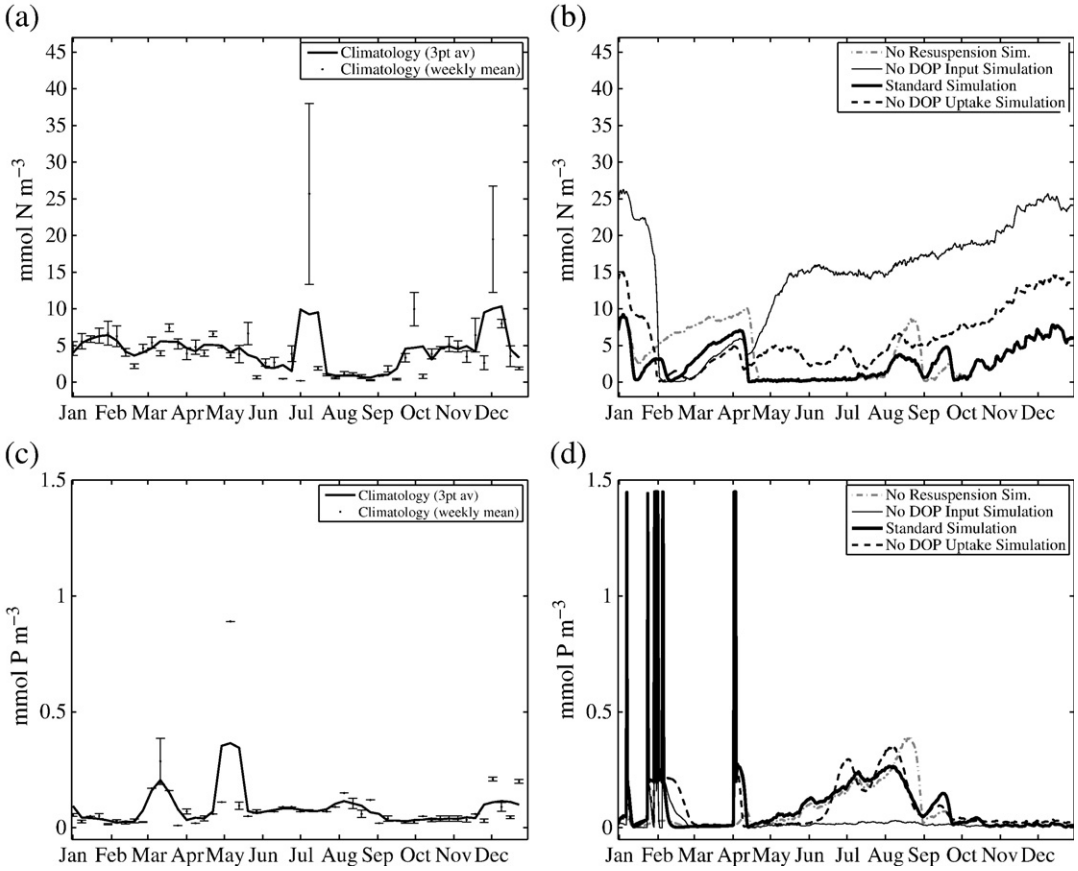

Fig. 4. Observed and modeled inorganic nutrients for four different simulations: *Standard simulation* (including DOP inputs and resuspension), *No Resuspension Simulation* (including DOP inputs but not resuspension), *No DOP Input Simulation* (including resuspension but not DOP inputs), and *No DOP Uptake Simulation* (including DOP inputs and resuspension, but not DOP uptake). (a) Observed DIN concentration. (b) Modeled DIN concentration. (c) Observed DIP concentration. (d) Modeled DIP concentration.

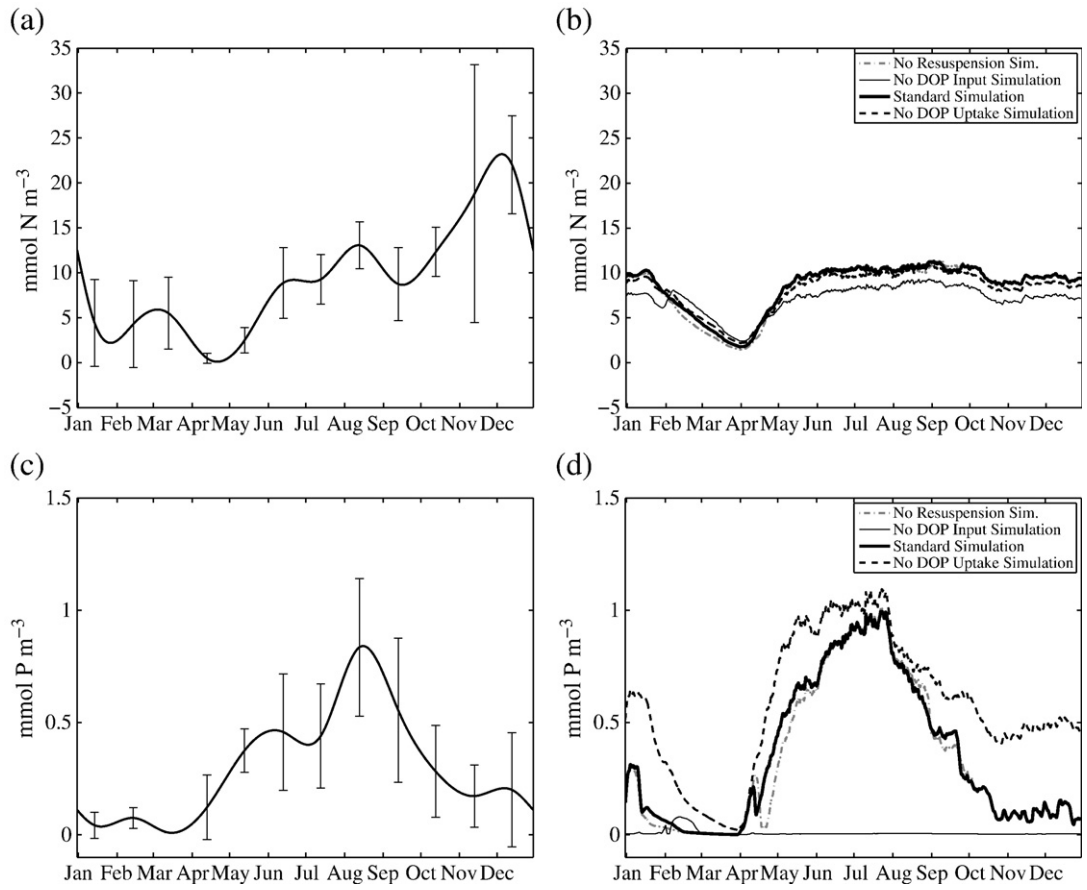

Fig. 5. Observed and modeled organic nutrients for four different simulations: *Standard simulation* (including DOP inputs and resuspension), *No Resuspension Simulation* (including DOP inputs but not resuspension), *No DOP Input Simulation* (including resuspension but not DOP inputs), and *No DOP Uptake Simulation* (including DOP inputs and resuspension, but not DOP uptake). (a) Observed DON (Redrawn from Loureiro et al. (2009)). (b) Modeled DON. (c) Observed DOP (Redrawn from Loureiro et al. (2009)). (d) Modeled DOP.

Simulation, and has been omitted from the figures, although some of its results will be commented below. There were no observational data for zooplankton or detritus, but the model outcomes are presented in Fig. 7.

3.1. Dissolved inorganic nutrients

Measured DIN concentrations (Fig. 4(a)) are variable, as can be seen from the large standard errors of the mean for some months. DIN concentrations tend to decrease during the summer months, but there are occasional peaks of more than 40 mmol N m^{-3}. The temporal evolution of the DIN concentrations for the five simulations (Fig. 4(b)) can be clustered into two groups. The *No DOP Input Simulation* and the *No Extra P Simulation* are characterized by values of DIN that exceed 15 mmol N m^{-3} during almost two thirds of the year. These two simulations differ only from February to April, when the *No DOP Input Simulation* gives DIN values lower than 5 mmol N m^{-3} while the minimum concentrations for the *No Extra P Simulation* (not shown) are always higher than 15 mmol N m^{-3}. The other three simulations, which include DOP input from the channels, show higher DIN in winter, fall and the beginning of spring, and lower DIN during the end of spring and summer. Among these, the simulations with DOP uptake (*No Resuspension Simulation* and *Standard Simulation*) present a more severe DIN depletion in the summer and lower DIN concentrations in the fall than the simulations with no DOP uptake. The range and temporal evolution of DIN concentration in these simulations with uptake of DOP agrees fairly well with the observations, although the *No Resuspension Simulation* shows a higher early spring maximum than the observations.

The modeled DIP values (Fig. 4(c)) are similar to the observations (Fig. 4(d)) in all the simulations except in those that do not include DOP inputs from the channels. The observations and the simulations with DOP inputs (*Standard Simulation*, *No Resuspension Simulation*, and *No DOP Uptake Simulation*) show a DIP maximum in the summer, when DIN is depleted, and low values in fall and winter. In contrast, the simulations without DOP input (*No DOP Input Simulation* and the *No Extra P Simulation*) show DIP concentrations lower than 0.05 mmol P m^{-3} during most of the year. The simulations that include resuspension (the *Standard Simulation*, the *No DOP Input Simulation*, and the *No DOP Uptake Simulation*) present some short events with DIP values reaching almost 1.5 mmol P m^{-3} at the beginning of February and April. Such peaks are not present in the observations, but given their short duration and the weekly sampling interval, they could easily have been missed.

3.2. Dissolved organic nutrients

The five simulations show the same pattern regarding DON concentrations (Fig. 5(b)), with a minimum around 3 mmol N m^{-3} in March. The observations (Fig. 5(c)) are of the same range. They also show a minimum in March, but rise from April to December, when there is a maximum of 20 mmol N m^{-3} characterized by high variability.

As for DIN, the modeled DOP results (Fig. 5(d)) fall in two groups, but only the results of the simulations including DOP input from the channels resemble the observations (Fig. 5(c)). The simulations that do not include DOP input (*No DOP Input Simulation* and *No Extra P Simulation*) lead to concentrations close to zero during most of the year, except for a small peak in February. The rest of the simulations

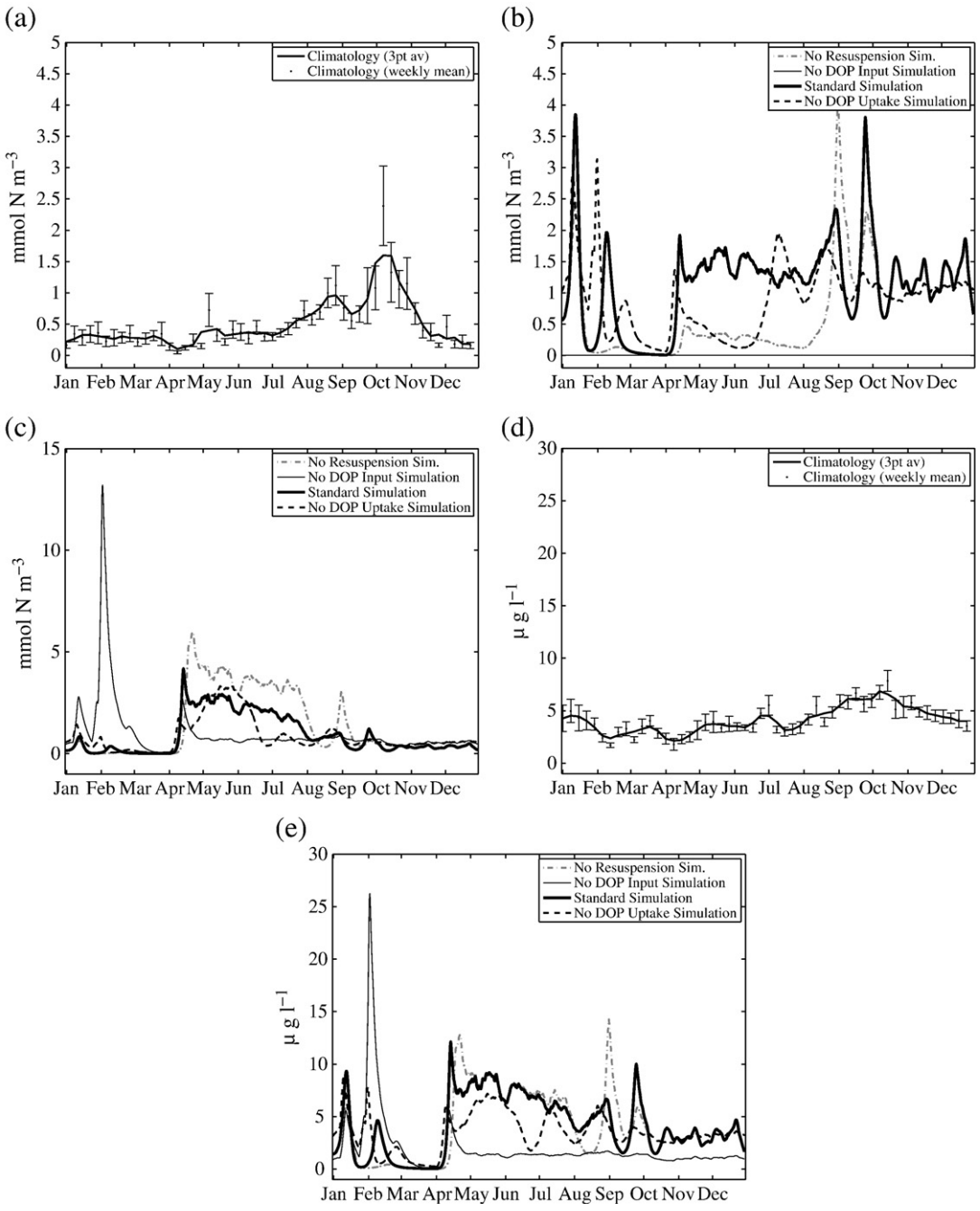

Fig. 6. Observed and modeled phytoplankton biomass and chlorophyll *a* for four different simulations: *Standard simulation* (including DOP inputs and resuspension), *No Resuspension Simulation* (including DOP inputs but not resuspension), *No DOP Input Simulation* (including resuspension but not DOP inputs), and *No DOP Uptake Simulation* (including DOP inputs and resuspension, but not DOP uptake). (a) Observed diatom concentration. (b) Modeled PH1 (diatom) concentration. (c) Modeled PH2 (flagellate) concentration. (d) Observed chlorophyll *a* concentration. (e) Modeled chlorophyll *a* concentration.

(*No Resuspension Simulation*, *Standard Simulation* and *No DOP Uptake Simulation*) show low values during the closed channel season, from January to March, and increase from March to reach a maximum of approximately 1 mmol P m^{-3} in July, followed by low DOP concentrations during the last three months of the year. The evolution of DOP in the *No DOP Uptake Simulation* is similar to that of the two simulations that include DOP inputs from channels, but with higher concentrations, particularly during the last months of the year.

3.3. Biological variables

According to the climatological data (Fig. 6(a)), diatom population density rises from January to October, when it reaches a peak of about 1.5 mmol N m^{-3}, although with high variability, and decreases from October to December. The three simulations (Fig. 6(b)) that include DOP input show a similar magnitude, variability, and some aspects of the general trend. In the *No DOP Uptake Simulation* and the *Standard Simulation* diatom biomass presents a minimum during the winter months and increases in spring months to values around 1.5 mmol N m^{-3} that last until December. The population density is more variable during autumn, in agreement with the observations (largest error standard deviation) and shows a peak of 4 mmol N m^{-3}. The *No Resuspension Simulation* shows the same trend as the *Standard Simulation*. The diatom abundance remains low (less than 0.5 mmol N m^{-3}) until July, and shows an earlier maximum than the other simulations and the measurements. In contrast, diatoms

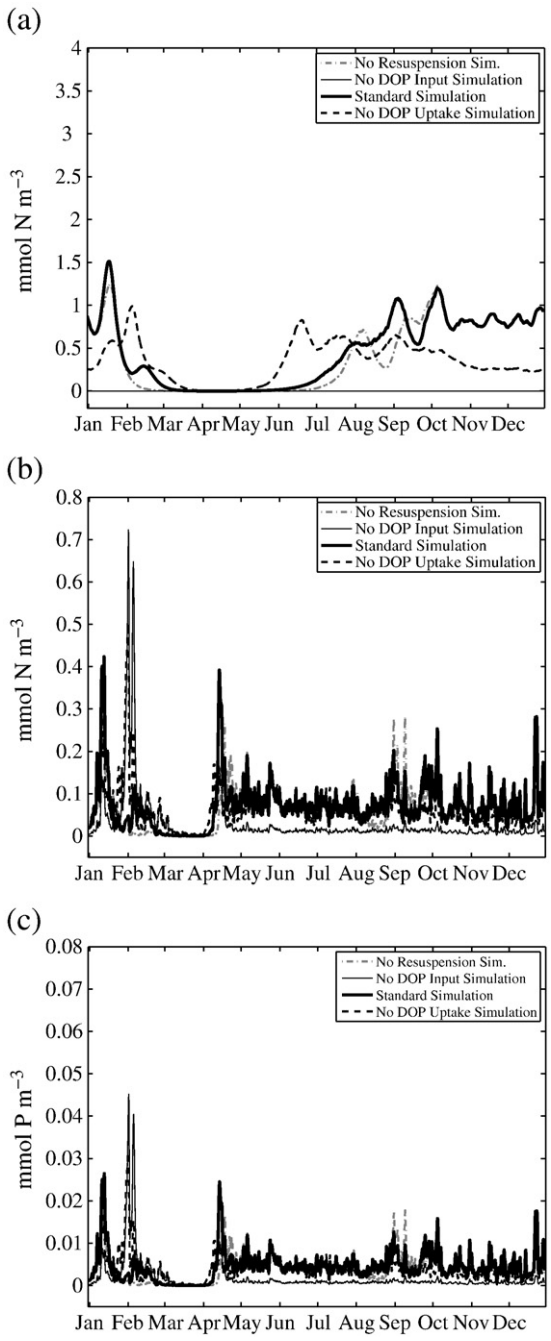

Fig. 7. Modeled zooplankton and detritus for four different simulations: *Standard simulation* (including DOP inputs and resuspension), *No Resuspension Simulation* (including DOP inputs but not resuspension), *No DOP Input Simulation* (including resuspension but not DOP inputs), and *No DOP Uptake Simulation* (including DOP inputs and resuspension, but not DOP uptake). (a) Zooplankton (ZOO). (b) Detrital nitrogen (DTN). (c) Detrital phosphorus (DTP).

were not able to grow (biomass equal zero mmol N m^{-3}) in the simulations without DOP inputs from the channels, in clear discrepancy with the observations. There were no significant differences between the *No DOP Input Simulation* and the *No Extra P Simulation*.

The modeled flagellate population densities (Fig. 6(c)) present a sharp increase when the channels open in April, with maxima of 6 mmol N m^{-3} (*No Resuspension Simulation*), 4 mmol N m^{-3} (*Standard Simulation*), and 3 mmol N m^{-3} (*No DOP Uptake simulation*). Flagellate abundances remain high during spring and early summer and decrease in late summer and fall while the diatom concentrations are still high. In the *No DOP Input Simulation* flagellates exhibit a high peak in February of almost 15 mmol N m^{-3} and seem to outcompete the diatoms that are unable to grow. However, such a high winter maximum has not been observed (de Pedro, 2007). This simulation also shows a small peak after closing of the channels in April.

The chlorophyll climatology (Fig. 6(d)) displays a minimum of 3 μg l^{-1} around February and March, and a maximum of 6 μg l^{-1} in October. The simulated chlorophyll (Fig. 6(e)) for the *Standard Simulation*, the *No Resuspension Simulation*, and the *No DOP Uptake Simulation* spans a larger range than the observed values, insofar as the minimum is too low because none of the modeled phytoplankton groups grows when the channels are closed. The range for the *No DOP Uptake Simulation* is similar, but the spring variability is higher than in the other simulations that include DOP input. The chlorophyll values of the simulations that do not include DOP inputs, i.e., *No DOP Input Simulation* and *No Extra P Simulation*, include a peak in February corresponding to the flagellate maximum and are low during the rest of the year, a pattern that differs from that of the other simulations and from the observations.

The zooplankton results (Fig. 7(a)) suggest, again, that the simulations not including DOP inputs (*No DOP Input Simulation* and *No Extra P Simulation*) are less realistic, as the zooplankton concentration goes to zero mmol N m^{-3}. The other simulations *(Standard Simulation*, *No Resuspension Simulation*, and *No DOP Uptake Simulation)* are the most realistic and present a similar trend with a minimum in spring and higher values the rest of the year. No data are available to validate these modeled results.

3.4. Detritus pools

The detritus pools of both nitrogen and phosphorus (Fig. 7(b) and (c)) follow the same pattern. The concentrations are relatively constant throughout the year, although all the simulations display a minimum at the end of March. From March to December, there is almost no detritus remaining in the mixed layer for the simulations that do not include DOP inputs. The detrital concentrations of the *No DOP Input Simulation* are roughly 10 times smaller than those of the other simulations for both phosphorus and nitrogen. The DTN and DTP concentrations for the *No Extra P Simulation* (data not shown) are similar to those of the *No DOP Input Simulation*, with slightly lower values during the first 50 days of the year.

3.5. Most limiting nutrient

Determining the most limiting nutrient for phytoplankton growth is not a straightforward process. As explained by Flynn (2010-this issue), the diagnostic factors for nutrient stress are cellular functions (such as the C:N:P ratio); therefore, nutrient concentrations in the environment and not their ratio are important. In the case of our model, which used a colimitation formulation (Eqs. (20) and (21)), the most limiting nutrient is the one for which the ratio of the half saturation constant to the nutrient concentration is largest, and therefore contributes the most to reduce the uptake coefficient. In the context of this work, we will consider only N and P, although Si exerts also some degree of limitation on PH1 (diatoms).

The DIN, the available phosphorus ($P = DIP + a_{(DOP)}DOP$ for the *Standard Simulation* and $P = DIP$ for the *No DOP Uptake Simulation*) and the uptake coefficient for diatoms (PH1) and flagellates (PH2) are displayed in Fig. 8. The results of the *No Resuspension Simulation* are qualitatively similar to the *Standard Simulation* and are not shown. The ratios $Ks_{DIN,PHX}/DIN$ and $Ks_{P,PHX}/P$ were calculated to determine the periods when DIN (solid lines at top of Fig. 8) or P (dashed lines at top of Fig. 8) is the most limiting nutrient.

In the *Standard simulation* (Fig. 8(a)), phosphorus appears as the most limiting nutrient during fall to early spring while nitrogen is the most limiting in late spring and summer. The fall phosphorus limitation is due to low DIP and DOP, and high nitrogen concentrations from the

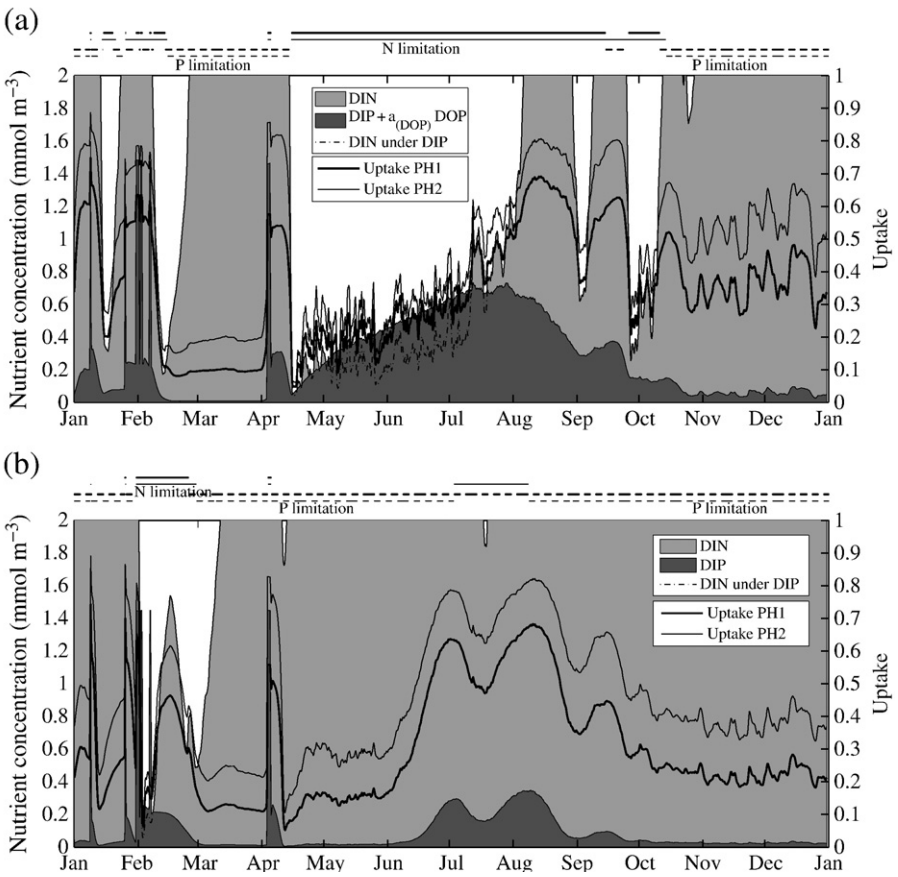

Fig. 8. (a) Concentrations of DIN and DIP + $a_{(DOP)}DOP$ in the *Standard Simulation*. (b) Concentrations of DIN and DIP in the *No DOP uptake Simulation*. Only the range 0–2 mmol m^{-3} is shown for nutrient concentration. The thick and thin lines in the graph indicate, respectively, the uptake by PH1 (diatoms) and PH2 (flagellates). The lines above the respective plots indicate the periods of nitrogen (thick solid line for diatom and thin solid line for flagellates) and phosphorus (thick dashed line for diatom and thin dashed line for flagellates) as most limiting nutrient. The most limiting nutrient was obtained by comparing the ratio of the half saturation constant to ambient concentration for each nutrient.

channel discharge. In winter, the channels are closed (no DOP) but groundwater discharge is high in DIN and low in DIP; nitrogen and phosphorus limitation alternate with high frequency. The high variability of sediment resuspension during that period leads to input of high DIP concentration in the water column, which reduces phosphorus limitation. The high DOP discharge in summer seems to alleviate phosphorus limitation. In the *No DOP Uptake Simulation* (Fig. 8 (b)), phosphorus limitation appears to be dominant for most of the year.

4. Sensitivity analysis to freshwater inputs

A sensitivity analysis was performed to evaluate the robustness of the model results. We believe that the largest uncertainty in this study resides in the freshwater inputs, i.e., channel and underground fluxes as well as their inorganic and organic concentrations. We, therefore, used a "one-at-a-time" methodology, which consists of varying one variable while holding the others fixed (Hamby, 1994; Fasham, 1995). The *Standard Simulation* was repeated by doubling and reducing by half the fluxes as well as the concentrations. That corresponds to the range that was found in the literature related to Alfacs Bay.

When perturbing the channel (Fig. 9) and underground (data not shown) nutrient concentrations, the temporal evolution of the modeled concentrations remains similar to the ones in the *Standard Simulation*, although their magnitudes change. More specifically, when the channel DOP is doubled, the DIP and DOP in the bay are doubled, the diatom concentration increases in the spring and their bloom lasts longer. When the channel DIN is doubled, DOP concentration remains low until early summer, DIN increases mainly in winter and fall but the summer depletion is still present. In that case, the flagellate bloom in spring lasts longer, and diatoms exhibit the highest variability in the summer instead of the fall. Raising the DIN in the underground channels has the same effect, although it is less accentuated. Reducing the channel DOP by half seems to have similar effect as doubling DIN in the channel. Doubling the underground DIP mainly affects the DIN concentration in the bay, which decreases, most notably in winter and fall. This addition also impacts the phytoplankton community composition, with an increase of diatoms and a decrease of flagellates in spring.

Perturbations of the channel and underground fluxes (data not shown), also conserve the trends of the *Standard Simulation*, while the nutrient concentrations change slightly in magnitude and peaks of short duration appear more frequently. The decrease of underground flow by half causes high variability in most of the variables in the bay, like the diatoms and flagellates (especially in summer and fall), the DIP concentration (which shows important peaks in summer) and the DIN concentration (which presents variability during the second part of the year). It also increases the concentration of organic nutrients. Doubling the underground flow has similar effects to doubling the DIN in the channels or in the underground flow. Doubling the channel flow has minor effect, except for a decrease of DIN and a switch between the diatom and flagellate dominance in spring similar to the one observed when increasing the phosphorus in the underground water.

The patterns of nitrogen or phosphorus limitation (not shown) are generally similar in all sensitivity experiments. Most cases show nitrogen as the most limiting nutrient in late spring and summer and phosphorus in the fall to early spring, although the length of the periods of limitation by nitrogen or phosphorus varies. The extreme cases are the simulations performed with half DOP or double DIN in the channels,

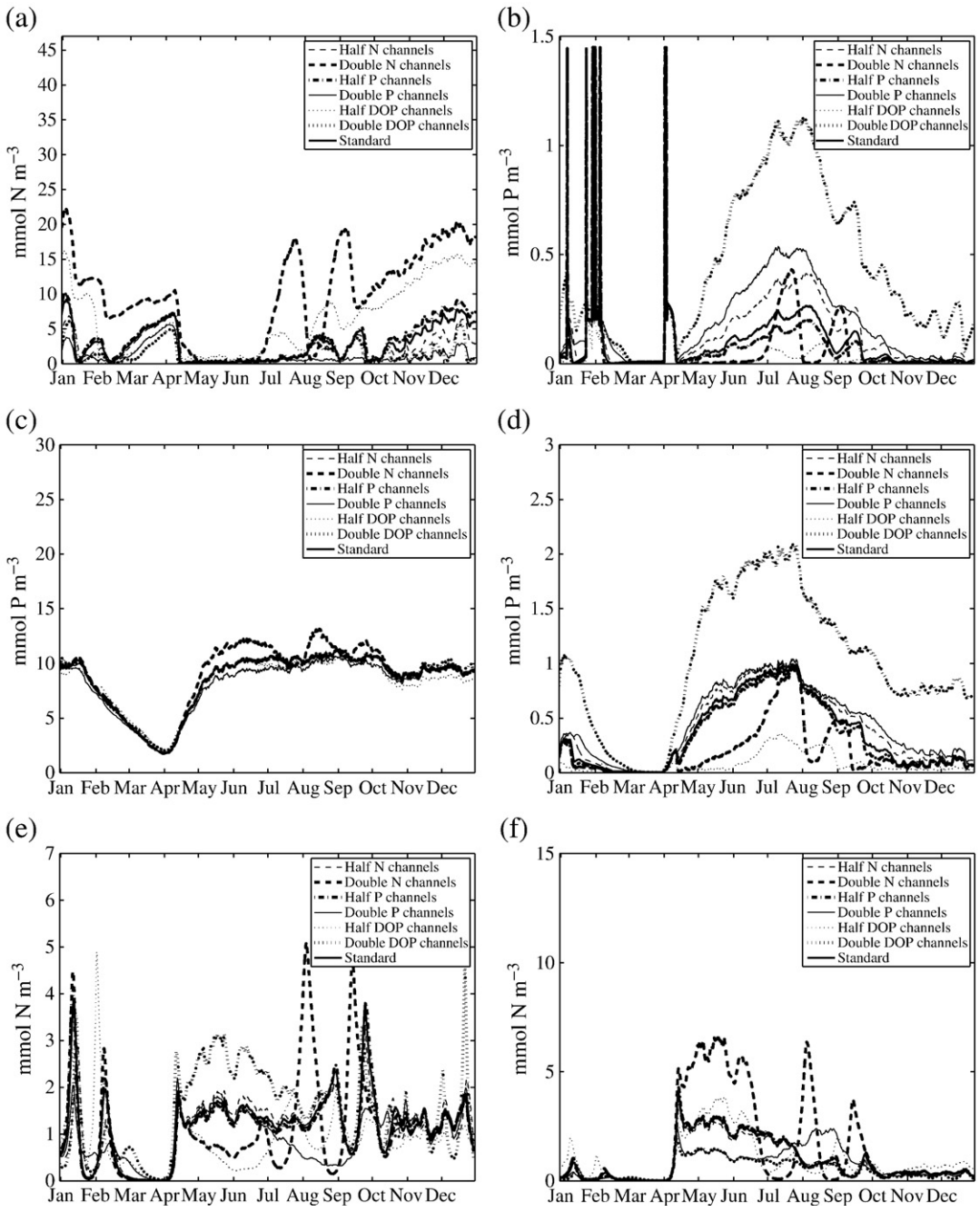

Fig. 9. Modeled results after doubling and reducing by half the nutrient concentration in the channels. (a) Dissolved Inorganic Nitrogen (DIN). (b) Dissolved Inorganic Phosphorus (DIP). (c) Dissolved Organic Nitrogen (DON). (d) Dissolved Organic Phosphorus (DOP). (e) Diatoms (PH1). (f) Flagellates (PH2).

in which the most limiting nutrient is phosphorus during most of the year, and the simulations with double DOP or half DIN, in which nitrogen limitation dominates most of the time. The time when phosphorus becomes the most limiting nutrient in the fall varies considerably among the experiments. In addition, the alternation between predominance of nitrogen or phosphorus limitation in January–February displays great variability.

5. Discussion

The ecological model presented here was designed with the aim of understanding the role played by different nutrient sources in the control of phytoplankton production in Alfacs Bay. As previously explained, our hypotheses were that there is an alternation in time between the dominance of limitation by nitrogen and phosphorus, and that, in addition to inorganic nutrient inputs from freshwater discharge and exchange with the sea, there are two additional processes that allow this alternation: P release by sediment resuspension and a DOP source from the channels that can be made available for phytoplankton growth either by remineralization and/or by direct uptake.

The results of the five considered simulations can be grouped into two categories: the first includes the simulations without DOP inputs from the channels (*No DOP Input Simulation* and *No Extra P Simulation*) and the second includes those with DOP input (*Standard Simulation*, *No DOP Uptake Simulation*, and *No Resuspension Simulation*). In the first category, the DIN, DIP and DOP concentrations during the summer reach values that are in marked disagreement with the observations. Similarly, diatom abundance and chlorophyll *a* deviate largely from the climatological observations. The second set of simulations leads to results that are in closer agreement with the temporal evolution of the

nutrients, chlorophyll *a*, and phytoplankton abundance. There are no data in Alfacs to compare with zooplankton, but the modeled ZOO ranges for the simulations that include DOP are similar to measured values in Mediterranean coastal areas (Calbet et al., 2001).

Based upon the model simulations, we suggest that in order to allow the observed phytoplankton development, there must be an extra source of phosphorus in addition to DIP. As shown in the results of the *No Extra P Simulation*, without this additional phosphorus, the organisms are not capable of drawing down the DIN. As a consequence, DIN remains too high, especially during the fall and winter period, and the diatoms, zooplankton and chlorophyll stay too low. Thus, our model shows evidence that DOP inputs from freshwater sources are a key process in the ecosystem dynamics of Alfacs Bay.

The idea that resuspension of sediments plays an important role in the ecosystem response (Vidal et al., 1992) appears to need some reconsideration. The resuspension mechanism introduces phosphorus into the water column, but the amount of phosphorus in the mixed layer from this resuspension is low compared with the other DIP sources. It is, therefore, not possible to explain the magnitude of observed variables by only taking into account the resuspension mechanism, and it is not possible to find substantial differences between a simulation that includes resuspension and a simulation that does not. We recognize that there are periods during which the concentrations of the mixed layer are influenced by the resuspension of sediment. These are the periods of closed channels, with lower DIN inflow. A small addition of phosphorus could then induce a switch in the nutrient limitation. During these months, the wind is stronger than in summer and the lack of freshwater discharge from the channels weakens the stratification, making it more favorable for sediment resuspension. The results of the model show that the closed channel period is the only period where the *No Extra P Simulation* and the *No DOP Input Simulation* differ, with higher PH1 and PH2 concentrations in the *No DOP Input Simulation*. Thus, we cannot discard the possibility that resuspension has a role during the closed channel months. In addition, there might be episodic events when particularly strong resuspension of sediments can bring larger amounts of phosphorus to the water column.

Sediment resuspension in Alfacs Bay (Guillén, 1992) can be caused by currents coming from the south and entering the bay through the mouth, and by wind stirring. The model considered only the latter mechanism, which is the most common (Guillén, 1992). Sediment resuspension could be more important during periods of high currents and therefore a full three-dimensional model with sediment resuspension would be necessary to accurately simulate the phosphorus input from the sediment. While the influence of sediment resuspension on DIP concentrations of the mixed layer was negligible, it is also possible that resuspension could affect the phosphorus and nitrogen pools of the deeper water layers. Finally, the load of phosphorus from sediments could be affected by episodes of anoxia, because the phosphorus is liberated in soluble form in anoxic environments (Golterman, 2001). Anoxia, however, rarely occurs in Alfacs Bay (Camp et al., 1991; de Pedro, 2007).

The concentrations of DOP in the bay range from 0 to 1.2 mmol m^{-3} (Loureiro et al., 2009), but the origin of this material is not well known. Loureiro et al. (2009) associated DOP input in Alfacs Bay with freshwater discharge. Forès (1989) and Forès (1992), studied nutrient fluxes in the rice fields of the Ebre Delta, and observed a release of DOP during several phases of rice growth, from April to mid July. According to the model, DOP input from channels is, indeed, the most important source of DOP to Alfacs, ahead of exudation and detritus remineralization.

This study points towards the importance of DOP for the ecosystem of Alfacs Bay. The similarity of the results of the simulations with or without DOP uptake by both groups of phytoplankton (*Standard Simulation* and *No DOP Uptake Simulation*, respectively), indicates that DOP remineralization to DIP, a process that can occur at relatively fast rates in aquatic systems (Lomas et al., 2010), plays a substantial role. However, the fact that the agreement with the observations is better in the *Standard Simulation* than in the *No DOP Uptake Simulation* supports the occurrence of direct DOP uptake by phytoplankton. A number of studies have reported the use of DOP by phytoplankton species of various groups, albeit at different degrees. In particular, it has been shown that some HAB-forming dinoflagellates like *Alexandrium tamarense* or *Prorocentrum minimum* (which are present in Alfacs) grow well on DOP. This ability could help them to outcompete other species and cause noxious outbreaks, particularly in situations of DIP depletion (Oh et al., 2002; Heil et al., 2005).

Our model simulations suggest that phosphorus tends to be more limiting at the beginning and end of the year (Fig. 8), when its inputs are low. The highest phosphorus loads, due to DOP, tend to occur between May and October. The relationships between half saturation to nutrient concentration ratios argue for predominance of nitrogen limitation during this period. A similar seasonal pattern was observed by Fisher et al. (1992) in Chesapeake Bay, who related it to changes in the composition of freshwater inputs. A comparison of Figs. 3(h) and 8 suggests that the main driver of the changes in nitrogen and phosphorus availability are the freshwater fluxes from the channels and their associated DOP inputs.

As found in other estuaries, the switch in limiting nutrients over the year is likely to affect phytoplankton biomass, composition and seasonal cycle (McComb et al., 1981; D'Elia et al., 1986; Fisher et al., 1992). N and P availability in general could also influence the biochemical composition of phytoplankton and could be important in relationship with food quality for grazers (Estrada et al., 2008). From a management point of view, the alternation of phosphate and nitrogen limitation suggests the need to control the inputs of both nutrients in order to avoid potential eutrophication problems.

The results of our modeling study also highlight some key aspects that need to be addressed to improve our understanding of the nutrient budgets and the ecosystem processes in Alfacs Bay. For example, the model did not take into account the possible contribution of dissolved organic nitrogen (DON) to phytoplankton growth (Berman and Bronk, 2003). This ability could, however, favor some taxa, as suggested by Loureiro et al. (2009) to explain *Pseudo-nitzschia* spp. dynamics. We also need to gain insight into allochthonous sources of DOP and into its metabolism in the planktonic community. Other sources of phosphorus coming from freshwater should also be considered, such as the presence of particulate organic phosphorus (POP) and particulate inorganic phosphorus (PIP). These have not been measured in detail in Alfacs, but some values given by Muñoz (1998) suggest that the amount of particulate phosphorus coming from freshwater ranges from 1.5 to 3.0 mmol P m^{-3}. The addition of this amount of particulate phosphorus (as detritus) into Alfacs Bay does not substantially change our conclusions due to the fact that the detrital matter sinks quite rapidly to the bottom. The concentration of PP would have to be more than one hundred times higher than the observations in order to see some effect in the model results (not shown). Finally, heterotrophic bacteria could play a role in the phosphorus cycle (Bentzen et al., 1992). In our model the remineralization rate was taken constant over time, but further studies are needed to better define this process. The zero-dimensional model presented here has been useful to test our hypotheses. However, more realistic simulations should take the presence of spatial variability into account, both in the water column (Delgado and Camp, 1987) and in the sediment (Vidal et al., 1992). Three-dimensional simulations would allow a more detailed analysis of the spatio-temporal variability of the studied ecosystem.

Given the importance of the freshwater discharges as illustrated in this study, it would be desirable to have long time series of flows and nutrient content of freshwater entering the bay, both from the drainage channels and from ground water discharges. According to Llebot (2007), who used a 3D free-surface hydrostatic model of water circulation in Alfacs Bay, the existence of substantial underground

water inputs was essential to explain the water column structure observed in winter. Given the potentially high nutrient concentrations in these waters it is important to better constrain their fluxes and composition.

6. Conclusions

We have used a simple ecological model to study the nutrient budget in a Mediterranean estuarine bay. Based on the simulation of five scenarios for Alfacs Bay involving the availability of DOP and its use by phytoplankton, and the presence or absence of DIP inputs from sediment resuspension, we suggest that DOP plays a key role in providing a phosphorus source that allows draw-down of nitrate and build-up of phytoplankton biomass. Sediment resuspension does not appear to be a significant source of phosphorus, although it could have some effect during the periods of low nitrogen load. The inclusion of DOP as a phosphorus source leads to an alternation between phosphorus (winter) and nitrogen (spring and summer) limitation. The limitation during fall switches from nitrogen to phosphorus depending on the amount of DOP delivered to the bay.

Acknowledgements

This work was funded by projects TURECOTOX (CTM2006-13884-CO2-00/MAR9, Ministerio de Ciencia e Innovacion, Spain) and CANESP (a joint project between the National Research Council of Canada and the Ministerio de Asuntos Exteriores of Spain), and by the CSIC. CL was supported by a fellowship of the Spanish National Research Council, CSIC (Beca CSIC Predoctoral I3P-BPD2005), and during the last months for a postgraduate grant of La Fundación Caja Madrid. The modeling was performed during CL's internship in the College of Oceanic and Atmospheric Sciences at Oregon State. We thank Tim Cowles for hosting CL during her first stay in the US and for his help and support during the first stages of the model development. JS was funded by Proyecto Intramural Especial del CSIC, "Desarrollo de algoritmos y validación de productos en el Centro Experto SMOS en Barcelona" (200430E530). We are grateful to Maximinio Delgado for kindly providing phytoplankton data, to Elisa Berdalet, Esther Garcés and Mariona Segura for valuable advice and information, and Francisco Rueda for his help during the process of implementation of the physical model Si3D to Alfacs. IRTA (Institut de Recerca i Tecnologia Agroalimentàries, Generalitat de Catalunya) sponsored the collection of time series of environmental data in Alfacs Bay. The Servei Meteorològic de Catalunya and the Instituto Nacional de Meteorología provided meteorological data. We also acknowledge the valuable comments of Annie Chapelle and an anonymous reviewer.

References

Aminot, A., Guillaud, J.F., Andrieux, F., 1993. Spéciation du phosphore et apports en baie de Seine orientale. Oceanol. Acta 16, 617–623.
Andrieux-Loyer, F., Aminot, A., 2001. Phosphorus forms related to sediment grain size and geochemical characteristics in french coastal areas. Estuar. Coast. Shelf Sci. 52, 617–629.
Arin, L., Anxelu, X., Moran, G., Estrada, M., 2002. Phytoplankton size distribution and growth rates in the Alboran Sea (SW Mediterranean): short term variability related to mesoscale hydrodynamics. J. Plankton Res. 24, 1019–1033.
Artigas, M.L., 2008. Estudi de la comunitat fitoplanctònica en relació amb la hidrodinàmica de la columna d'aigua a la badia dels Alfacs (NO Mediterrani). Master's thesis. Universitat de Barcelona.
Bentzen, E., Taylor, W.D., Millard, E.S., 1992. The importance of dissolved organic phosphorus to phosphorus uptake by limnetic plankton. Limnol. Oceanogr. 37, 217–231.
Berman, T., Bronk, D.A., 2003. Dissolved organic nitrogen: a dynamic participant in aquatic ecosystems. Aquat. Microb. Ecol. 31, 279–305.
Boyle, D.R., 1994. Design of a seepage meter for measuring groundwater fluxes in the nonlittoral zones of lakes — evaluation in a boreal forest lake. Limnol. Oceanogr. 39, 670–681.
Brainerd, K.E., Cregg, M.C., 1995. Surface mixed and mixing layer depths. DSR 42, 1521–1543.
Calbet, A., Garrido, S., Saiz, E., Alcaraz, M., Duarte, C.M., 2001. Annual zooplankton succession in coastal NP Mediterranean waters: the importance of the smaller size fractions. J. Plankton Res. 23, 319–331.
Camp, J., 1994. Aproximaciones a la dinámica ecológica de una bahía estuárica mediterránea. Ph.D. thesis. Universitat de Barcelona.
Camp, J., Delgado, M., 1987. Hidrografía de las bahías del delta del ebro. Inv.Pesq. 51, 351–369.
Camp, J., Romero, J., Pérez, M., Vidal, M., Delgado, M., Martínez, A., 1991. Production–consumption budget in an estuarine bay: how anoxia is prevented in a forced system. Oceologia Aquatica 10, 145–152.
Chapelle, A., Ménesguen, A., Deslous-Paoli, J.M., Souchu, P., Mazouni, N., Vaquer, A., Millet, B., 2000. Modelling nitrogen, primary production and oxygen in a Mediterranean lagoon. Impact of oysters farming and inputs from the watershed. Ecol. Model. 127, 161–181.
Chen, C., Ji, R., Schwab, D.J., Beletsky, D., Fahnenstiel, G.L., Jiang, M., Johengen, T.H., Vanderploeg, H., Eadie, B., Budd, J.W., Bundy, M.H., Gardner, W., Cotner, J., Lavrentyev, P.J., 2002. A model study of the coupled biological and physical dynamics in lake michigan. Ecol. Model. 152, 145–168.
Crispi, G., Crise, A., Solidoro, C., 2002. Coupled mediterranean ecomodel of the phosphorus and nitrogen cycles. J. Mar. Syst. 33–34, 497–521.
Cruzado, A., Velásquez, Z., del Carmen Pérez, M., Bahamón, N., Grimaldo, N.S., Ridolfi, F., 2002. Nutrient fluxes from the ebro river and subsequent across-shelf dispersion. Cont. Shelf Res. 22, 349–360.
Currie, D.J., Kalff, J., 1984. A comparison of the abilities of freshwater algae and bacteria to acquire and retain phosphorus. Limnol. Oceanogr. 29, 298–310.
D'Elia, C.F., Sanders, J.G., Boynton, W.R., 1986. Nutrient enrichment studies in a coastal plain estuary: phytoplankton growth in large-scale continuous cultures. Can. J. Fish. Aquat. Sci. 43, 397–406.
DAAAR, 2008. Estadística de producció d'aqüicultura 2008. Departament d'Agricultura, Alimentació i Acció Rural, Generalitat de Catalunya.
de Pedro, X., 2007. Anoxic situations in estuarine zones without tidal forcing. An approach to the oxygen production/consumption budgets. Ph.D. thesis. Ecology department, University of Barcelona, Barcelona.
Delgado, M., Camp, J., 1987. Abundancia y distribución de nutrientes orgánicos disueltos en las bahías del delta del Ebro. Inv.Pesq. 51, 527-441.
Delgado, M., Estrada, M., Camp, J., Fernández, J.V., Santmartí, M., Lletí, C., 1990. Development of a toxic *Alexandrium minutum* Halim (Dinophyceae) bloom in the harbour of Sant Carles de la Ràpita (Ebro Delta, Northwestern Mediterranean). Sci. Mar. 54, 1–7.
Estrada, M., Sala, M.M., van Lenning, K., Alcaraz, M., Felipe, J., Veldhuis, M.J.W., 2008. Biological interactions in enclosed plankton communities including *Alexandrium catenella* and copepods: role of phosphorus. J. Exp. Mar. Biol. Ecol. 355, 1–11.
Farnós, A., Ribas, X., Reverté, J.T., 2007. El Canal Porta Vida. Exhibition, Museu Comarcal del Montsià.
Fasham, M., 1995. Variations in the seasonal cycle of biological production in subarctic oceans: a model sensitivity analysis. Deep-Sea Res. 42, 1111–1149.
Fasham, M.J.R., Ducklow, H.W., McKelvie, S.M., 1990. A nitrogen-based model of plankton dynamics in the oceanic mixed layer. J. Mar. Res. 48, 591–639.
Fennel, W., Neumann, T., 2004. Introduction to the Modelling of Marine Ecosystems. Elsevier. illustrated edition.
Fennel, K., Spitz, Y., Letelier, R.M., Abbott, M.R., Karl, D.M., 2002. A deterministic model for N_2 fixation at stn. ALOHA in the subtropical North Pacific Ocean. DSR2 49, 149–174.
Fernández-Tejedor, M., Soubrier-Pedreño, M.A., Furones, M.D., 2004. Acute LD_{50} of a *Gyrodinium corsicum* natural population for *Sparus aurata* and *Dicentratchus labrax*. Harmful Algae 3, 1–9.
Fisher, H.B., List, E.J., Koh, R.C.Y., Imberger, J., Brooks, N.H., 1979. Mixing in Inland and Coastal Waters. Academic Press.
Fisher, T.R., Peele, E.R., Ammerman, J.W., Harding, L.W., 1992. Nutrient limitation of phytoplankton in Chesapeake Bay. Mar. Ecol. Prog. Ser. 82, 51–63.
Flynn, K.J., 2010. Do external resource ratios matter? Implications for modelling eutrophication events and controlling harmful algal blooms. Journal of Marine Systems 83, 170–180.
Forès, E., 1989. Ricefields as filters. Arch. Hydrobiol. 116, 517–527.
Forès, E., 1992. Nutrient loading and drainage channel response in a ricefield system. Hydrobiological 230, 193–200.
Forès, E., Comín, F.A., 1992. Ricefields, a limnological perspective. Limnetica 10, 101–109.
Franks, P.J.S., 2002. NPZ models of plankton dynamics: their construction, coupling to physiscs and application. J. Oceanogr. 58, 379-378.
Froelich, P.N., 1988. Kinetic control of dissolved phosphate in natural rivers and estuaries. Limnol. Oceanogr. 33, 649–668.
Garcés, E., Delgado, M., Camp, J., 1997. Phased cell division in a natural population of *Dinophysis sacculus* and the *in situ* measurement of potential growth rate. J. Plankton Res. 19, 2067–2077.
Garcés, E., Delgado, M., Masó, M., Camp, J., 1999. *In situ* growth rate and distribution of the ichthyotoxic dinoflagellate *Gyrodinium corsicum* paulmier in an estuarine embayment (Alfacs Bay, NW Mediterranean Sea). J. Plankton Res. 21, 1977–1991.
Giraud, X., 2006. Modelling an alkenone-like proxy record in the nw african upwelling. Biogeosciences 3, 251–269.
Golterman, H.L., 2001. Phosphate release from anoxic sediments or "what did mortimer really write?". Hydrobiological 450, 99–106.
Guillén, J., 1992. Dinámica y balance sedimentario en los ambientes fluvial y litoral del Delta del Ebro. Ph.D. thesis. Universitat Politècnica de Catalunya.
Hamby, D.M., 1994. A review of techniques for parameter sensitivity analysis of environmental models. Environ. Monit. Assess. 32, 135–154.

Heil, C.A., Glibert, P.M., Fan, C., 2005. *Prorocentrum minimum* (pavillard) Schiller. A review of a harmful algal bloom species of growing worldwide importance. Harmful Algae 4, 449–470.
Hernández, I., Pérez-Pastor, A., Lloréns, J.L.P., 2000. Ecological significance of phosphomonoesters and phosphomonoesterase activity in a small Mediterranean river and its estuary. Aquat. Ecol. 34, 107–117.
Huang, B., Hong, H., 1999. Alkaline phosphatase activity and utilization of dissolved organic phosphorus by algae in subtropical coastal waters. Mar. Pollut. Bull. 39, 205–211.
Jassby, A.D., Platt, T., 1976. Mathematical formulation of the relationship between photosynthesis and light for phytoplankton. Limnol. Oceanogr. 21, 540–547.
Johannes, R.E., 1964. Uptake and release of dissolved organic phosphorus by representatves of a coastal marine ecosystems. Limnol. Oceanogr. 9, 224–234.
Kishi, M.J., Kashiwai, M., Ware, D.M., Megrey, B.A., Eslinger, D.L., Werner, F.E., Noguchi-Aita, M., Azumaya, T., Fujii, M., Hashimoto, S., Huang, D., Iizumi, H., Ishida, Y., Kang, S., Kantakov, G.A., cheol Kim, H., Komatsu, K., Navrotsky, V.V., Smith, S.L., Tadokoro, K., Tsuda, A., Yamamura, O., Yamanaka, Y., Yokouchi, K., Yoshie, N., Zuenko, J.Z.Y.I., Zvalinsky, V.I., 2007. NEMURO — a lower trophic level model for the North Pacific marine ecosystem. Ecol. Model. 202, 12–25.
Lacroix, G., Nival, P., 1998. Influence of meteorological variabilitu on primary production dynamics in the Ligurian Sea (NW Mediterranean Sea) with a 1D hydrodynamic/biological model. J. Mar. Syst. 16, 23–50.
Lancelot, C., Spitz, Y., Gypens, N., Ruddick, K., Becquevort, S., Rousseau, V., Lacroix, G., Billen, G., 2005. Modelling diatom and *Phaeocystis* blooms and nutrient cycles in the southern bight of the North Sea: the Miro Model. Mar. Ecol. Prog. Ser. 289, 63–78.
le Quéré, C., Harrison, S.P., Prentice, I.C., Buitenhuis, E.T., Aumont, O., Bopp, L., Claustre, H., Cunha, L.C.D., Geider, R., Giraud, X., Klaas, C., Kohfeld, K.E., Legendre, L., Manizza, M., Platt, T., Rivkin, R.B., Sathyendranath, S., Uitz, J., Watson, A., Wolf-Gladrow, D., 2005. Ecosystem dynamics based on plankton functional types for global ocean biogeochemistry. Glob. Change Biol. 11, 2016–2040.
Lebo, M.E., 1991. Particle-bound phosphorus along an urbanized coastal plain estuary. Mar. Chem. 34, 225–246.
Lima, I.D., Olson, D.B., Doney, S.C., 2002. Intrinsic dynamics and stability properties of size-structured pelagic ecosystem models. J. Plankton Res. 24, 533–556.
Llebot, C., 2007. Hydrodynamic characterization of a Mediterranean bay using Si3D, a three-dimensional model for estuarine circulation. Master's thesis. Universidad de las Palmas de Gran Canaria.
Llebot, C., Delgado, M., Turiel, A., Fernández-Tejedor, M., Diogène, J., Camp, J., Solé, J., Estrada, M., 2008. Coupling phytoplankton and hydrography in Alfacs Bay using principal component analysis and empirical mode decomposition. European Geosciences Union. General Assembly 2008. Poster.
Llebot, C., Rueda, F., Solé, J., Estrada, M., 2009. Stratification and Mixing in Dynamics in a Mediterranean Estuarine Bay. ASLO Aquatic Sciences Meeting. Poster.
Lomas, M.W., Burke, A.L., Lomas, D.A., Bell, D.W., Shen, C., Dyhrman, S.T., Ammerman, J.W., 2010. Sargasso Sea phosphorus biogeochemistry: an important role for dissolved organic phosphorus (DOP). Biogeosciences 7, 695–710.
Loureiro, S., Garcés, E., Fernández-Tejedor, M., Vaqué, D., Camp, J., 2009. *Pseudo-nitzschia* spp. (Bacillariophyceae) and dissolved organic matter (DOM) dynamics in the Ebro Delta (Alfacs Bay, NW Mediterranean Sea). Estuar. Coast. Shelf Sci. 83, 539–549.
Mallo, S., Vallespinós, F., Ferrer, S., Vaqué, D., 1993. Microbial activities in estuarine sediments (Ebro Delta, Spain) influenced by organic matter influx. Sci. Mar. 57, 31–40.
McComb, A.J., et al., 1981. Eutrophication in the Peel–Harvey estuarine system, western Australia. In: Neilson, B.J., Cronin, L.E. (Eds.), Estuaries and Nutrients. N. J. Cifton and Humana Press, pp. 323–342.
Merico, A., Tyrrell, T., Lessard, E.J., Oguz, T., Stabeno, P.J., Zeeman, S.I., Whitledge, T.E., 2004. Modelling phytoplankton succession on the Bering Sea shelf: role of climate influences and trophic interactions in generating *Emiliana huxleyi* blooms 1997–2000. DSR 51, 1803–1826.
Ministerio de Obras Públicas, Transportes y Medio Ambiente; Ministerio de Industria y Energía, 1995. Libro blanco de las aguas subterráneas.
Monbet, P., McKelvie, I.D., Worsfold, P.J., 2009. Dissolved organic phosphorus speciation in the waters of the Tamar estuary (SW England). Geochim. Cosmochim. Acta 73, 1027–1038.
Muñoz, I., 1998. Carbono, nitrógeno y fósforo en la parte baja del río Ebro y en los canales de riego del Delta. Oceologia Aquatica 11, 23–25.
Némery, J., Garnier, J., 2007. Typical features of particulate phosphorus in the Seine estuary (France). Hydrobiological 588, 271–290.
O'Neill, R.V., DeAngelis, D.L., Pastor, J.J., Jackson, B.J., Post, W.M., 1989. Multimple nutrient limitations in ecological models. Ecol. Model. 46, 174-163.
Oh, S.J., Yamamoto, T., Kataoka, Y., Matsuda, O., Matsuyama, Y., Kotani, Y., 2002. Utilization of dissolved organic phosphorus by the two toxic dinoflagellates *Alexandrium tamarense* and *Gymnodinium catenatum* (dinophyceae). Fish. Sci. 68, 416–424.
Pinazo, C., Marsaleix, P., Millet, B., Estournel, C., Véhil, R., 1996. Spatial and temporal variability of phytoplnkton biomass in upwelling areas of the northwestern Mediterranean: s coupled physical and biogeochmical modelling approach. JMS 7, 161–191.
Platt, T., Callegos, C.L., Harrison, W.G., 1980. Photoinhibition of photosynthesis in natural assemblages of marine phytoplankton. J. Mar. Res. 38, 687–701.
Quijano-Sheggia, S., Garcés, E., Flo, E., Fernández-Tejedor, M., Diogène, J., Camp, J., 2008. Bloom dynamics of the genus *Pseudo nitzschia* (Bacillariophyceae) in two coastal bays (NW Mediterranean Sea). Sci. Mar. 72, 577–590.
Rueda, F.J., Cowen, E.A., 2005. The residence time of a freshwater embayment connected to a large lake. LO 50, 1638–1653.
Rueda, F.J., Schladow, S.G., Monismith, S.G., Stacey, M.T., 2003a. Dynamics of large polymictic lake. I: Field observations. J. Hydraul. Eng. 129, 82–91.
Rueda, F.J., Schladow, S.G., Pálmarsson, S.O., 2003b. Basin-scale internal wave dynamics during a winter cooling period in a large lake. J. Geophys. Res. 108.
Ruttenberg, K.C., 2001. Phosphorus cycle. In: Steele, J.H. (Ed.), Encyclopedia of Ocean Sciences. Academic Press, Oxford, pp. 2149–2162.
Salat, J., Garcia, M.A., Cruzado, A., Palanques, A., Arin, L., Gomis, D., Guillén, J., de León, A., Puigdefàbregas, J., Sospedra, J., Velásquez, Z.R., 2002. Seasonal changes of water mass structure and shelf slope exchanges at the Ebro Shelf (NW Mediteranean). Cont. Shelf Res. 22, 327–348.
Segura, M., 2007. Relació entre la distribució de nutrients i oxigen dissolt i la composició elemental del fitoplàncton a la Mar Catalana (N–O Mar Mediterrània). Ph.D. thesis. Universitat Politècnica de Catalunya.
Smith, E.L., 1936. Photosynthesis in relation to light and carbon dioxide. Proc. Natl. Acad. Sci. 22, 504–511.
Smith, P.E., 2006. A semi-implicit, three-dimensional model for estuarine circulation. Open-File report 2006–1004. U.S. Geological Survey.
Smith, C.G., Cable, J.E., Martin, J.B., M.R., 2008. Evaluating the source and seasonality of submarine groundwater discharge using a radon-222 pore water transport model. Earth Planet. Sci. Lett. 273, 312–322.
Solé, J., Turiel, A., Estrada, M., Llebot, C., Blasco, D., Camp, J., Delgado, M., Fernández-Tejedor, M., Diogène, J., 2009. Climatic forcing on hydrography of a Mediterranean bay (Alfacs Bay). Cont. Shelf Res. 29, 1786–1800.
Spitz, Y.H., Moisan, J.R., Abbott, M., 2001. Configuring an ecsystem model using data from the Bermuda Atlantic Time Series (BATS). DSR2 48, 1733–1768.
Stalker, J.C., Price, R.M., Swart, P.K., 2009. Determining spatial and temporal inputs of freshwater, including submarine groundwater discharge, to a subtropical estuary using geochemical tracers, Biscayne Bay, South Florida. Estuaries Coasts 32, 694–708.
Taft, J.L., Taylor, W.R., McCarthy, J.J., 1975. Uptke and release pf phosphorus by phytoplankton in the Chesapeake Bay Estuary, USA. Mar. Biol. 33, 21–32.
Torrecilla, N.J., Galve, J.P., Zaera, L.G., Retamar, J.F., Álvarez, A.N., 2005. Nutrient sources and dynamics in a Mediterranean fluvial regime (Ebro River, NE Spain) and their implications for water management. J. Hydrol. 304, 166–182.
Tyrrell, T., 1999. The relative influences of nitrogen and phosphorus on oceanic primary production. Nature 400, 525–531.
van den Berg, A.J., Ridderinkhof, H., Riegman, R., Ruardij, P., Lenhart, H., 1995. Influence of variability in water transport on phytoplankton biomass and composition in the southern North Sea: a modelling apporach (FYFY). Cont. Shelf Res. 16, 907–931.
Vidal, M., 1994. Phosphate dynamics tied to sediment disturbances in Alfacs Bay (NW Mediterranean). Mar. Ecol. Prog. Ser. 110, 211–221.
Vidal, M., Morguí, J., Latasa, M., Romero, J., Camp, J., 1992. Factors controlling spatial variability in ammonium release within an estuarine bay (Alfacs Bay, Ebro Delta, NW Mediterranean). Hydrobiological 235/236, 519–525.
Vidal, M., Morguí, J.A., Latasa, M., Romero, J., Camp, J., 1997. Factors controlling seasonal variability of benthic ammonium release oxygen uptake in Alfacs Bay (Ebro Delta, NW Mediterranean). Hydrobiological 350, 169–178.
Vila, M., Garcés, E., Masó, M., Camp, J., 2001. Is the distribution of the toxic dinoflagellate *Alexandrium catenella* expanding along the NW Mediterranean coast? Mar. Ecol. Prog. Ser. 222, 73–83.
Yamamoto, T., Oh, S.J., Kataoka, Y., 2004. Growth and uptake kinetics for nitrate, ammonium and phosphate by the toxic dinoflagellate *Gymnodinium catenatum* isolated from Hiroshima Bay. Jpn. Fish. Sci. 70, 108–115.